A NOVEL USE OF SAMPLING PRESSURE FROM SIDESTREAM CAPNOMETER

by

Veena Kaustaban

A thesis submitted to the faculty of
The University of Utah
in partial fulfillment of the requirements for the degree of

Master of Science

Department of Bioengineering

The University of Utah

December 2014

The University of Utah Graduate School

STATEMENT OF THESIS APPROVAL

The thesis of **Veena Kaustaban**

has been approved by the following supervisory committee members:

Joseph A. Orr	, Chair	**04/08/2014** Date Approved
Lara M. Brewer	, Member	**04/08/2014** Date Approved
Robert S. MacLeod	, Member	**04/08/2014** Date Approved

and by **Patrick A. Tresco** , Chair/Dean of

the Department/College/School of **Bioengineering**

and by David B. Kieda, Dean of The Graduate School.

ABSTRACT

Amplitude and shape of the respiratory carbon dioxide (CO_2) signal (capnogram) are not always a true reflection of the patient's respiratory status, especially during delivery of supplemental oxygen (O_2), and can result in false alarms. The goal of the project was to provide a more reliable source of patient monitoring and diagnosis by using the respiratory pressure signal to detect breaths in the presence of supplemental O_2. The Respironics LoFlo sidestream capnometer was used in the project to record the two signals. In preliminary tests, it was observed that the sampling pressure obtained from the capnometer was analogous to respiratory pressure and was hence used in analysis as its representative. The sampling flow signal was also acquired from the LoFlo system and studied.

The aforementioned signals were recorded from 4 human volunteers who had 100% O_2 or air delivered through a nasal cannula. The end-tidal CO_2 ($etCO_2$) was 2 ± 0.4 % lower, the sampling pressure and the sampling flow were 3 ± 0.9 times and 4.7 ± 1.2 times greater in amplitude, respectively, with O_2, than their corresponding values with air. Another finding in the presence of O_2 was the occurrence of double peaks in the pressure signal during expiration. It was hypothesized that O_2, being more viscous than air, caused the capnometer to behave differently in its presence. This was confirmed by a series of bench experiments. Clinical data were collected from patients undergoing colonoscopy with supplemental O_2 delivered at 6 liters per minute (LPM). The first step

in analysis was detection of O_2 from the pressure signal so that any observed double peak is accounted for and the amplitude of the signal is not misinterpreted. Breath rate was then calculated from the CO_2 and pressure signals and episodes of apnea were detected. The pressure and CO_2 signals detected 99% and 98% of apneic events, respectively, with a respective specificity of 100% and 99%. When considered individually, both signals had a sensitivity of 96%. The pressure signal resulted in 60% fewer false positive results than the CO_2 signal, thus greatly reducing the rate of false alarms. The pressure signal, being instantaneous, also detected respiratory effort before the capnogram. It is concluded that the sampling pressure signal can provide more reliable and accurate respiratory information than the capnogram.

TABLE OF CONTENTS

ACKNOWLEDGMENTS

I would like to thank my committee members, Joseph Orr, Lara Brewer, Robert MacLeod, and Vladimir Hlady, for their guidance and support. I sincerely thank Dwayne Westenskow for giving me the opportunity to work in the lab. I wish to express my love and gratitude to my parents, Kaustaban and Jeysree, for the countless sacrifices they have made for me. Thanks to Sheela for her constant encouragement. I dedicate my dissertation to Vikram Kaustaban, for always believing in me more than I believe in myself and without whom this would not be possible.

CHAPTER 1

INTRODUCTION

1.1 Capnography

1.1.1 Terminology and Definitions

Capnography is the noninvasive measurement of partial pressure of carbon dioxide (CO_2) in exhaled breath. A capnometer is a monitor that measures and displays changes in the CO_2 concentration during the respiratory cycle. The pictorial representation of the measured concentration is called the capnogram. Capnometers are designed in two configurations- mainstream and sidestream. A mainstream capnometer measures the amount of CO_2 directly from the airway, with the sensor located on the endotracheal tube (ET). This is different from a sidestream capnometer that aspirates a small sample from the exhaled breath through tubing, to a sensor located inside the monitor. The general construction of a mainstream and sidestream capnometer is depicted in Figures 1 and 2, respectively.

A normal capnogram is trapezoidal and can be divided into four phases depending on the stage of respiration during which it is recorded. At the beginning of expiration (phase-I), the CO_2-free airway dead space is cleared and CO_2 concentration is zero. As the dead space begins to mix with the alveolar gas, a steep rise in the CO_2 concentration

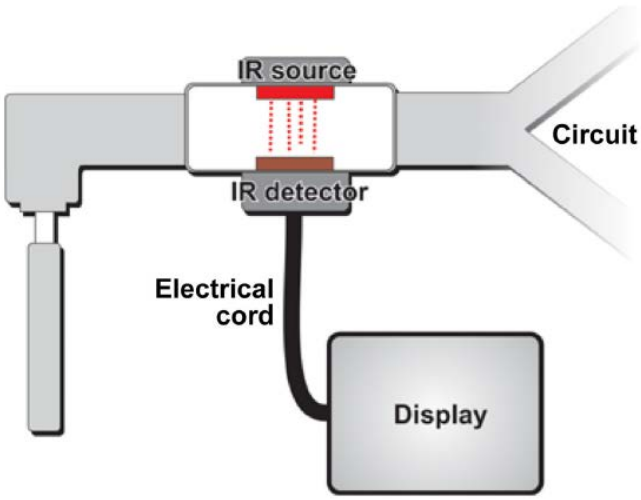

Figure 1: General construction of a mainstream capnometer. [1] The mainstream capnometer is characterized by measuring the concentration of CO_2 directly from the subject's airway as shown in the figure.

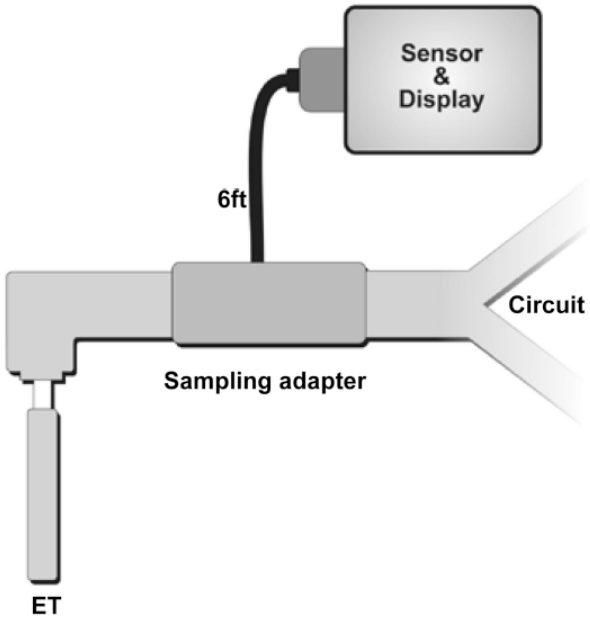

Figure 2: General construction of a sidestream capnometer. [1] In a sidestream capnometer, the sample is drawn away from the subject and the measurement system is located within the monitor, away from the patient.

occurs (phase-II). As the alveolar gas continues to be exhaled, the CO_2 concentration remains relatively constant (phase-III) and this phase is called the alveolar plateau. At the end of expiration, the CO_2 concentration is maximal and is called end-tidal CO_2 ($etCO_2$). As inhalation starts, CO_2 concentration drops to zero (phase-IV) and remains at baseline (phase-1) during inspiration and the cycle repeats. The different stages are labelled in a normal capnogram shown in Figure 3.

1.1.2 Principle of CO_2 Concentration Measurement

Most capnometers rely on infrared (IR) technology to detect and measure CO_2. The IR part of the electromagnetic spectrum extends from 0.7 μm to approximately 40 μm. CO_2 has a strong absorption band between 4.2 μm and 4.6 μm as shown in Figure 4. The peak absorption takes place at 4.26 μm. Nitrous oxide (N_2O) and water vapor also have absorption bands in this region of the spectrum. The collision between CO_2 and the oxygen in these molecules causes CO_2 to absorb more IR than it normally would, leading to an erroneous measurement. This is called collision broadening and can be removed by using appropriate filters. [2] The amount of IR light absorbed by the gas depends on the amount of CO_2. This follows the Beer-Lambert Law, described by Equation (1), according to which the emergent IR intensity is exponentially proportional to the concentration of the sampled gas-

$$I = I_o e^{-\mu C L} \qquad (1)$$

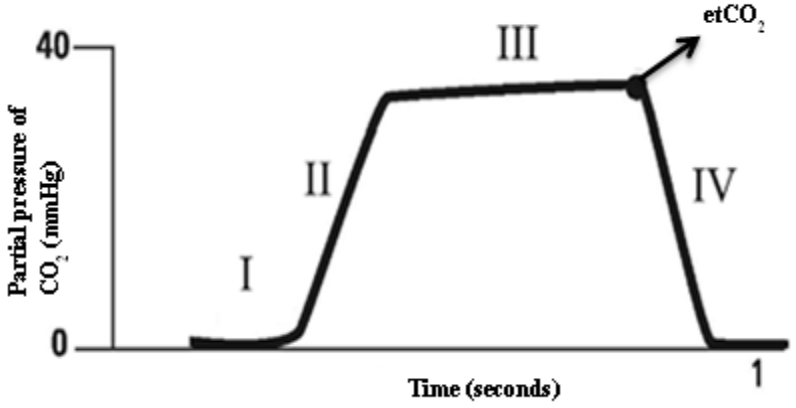

Figure 3: A normal capnogram. Shown in the figure are variations in the partial pressure of CO_2 during different phases of breathing, marked by Roman numerals. The peak partial pressure is observed at the end of expiration and is referred to as end-tidal CO_2 or $etCO_2$.

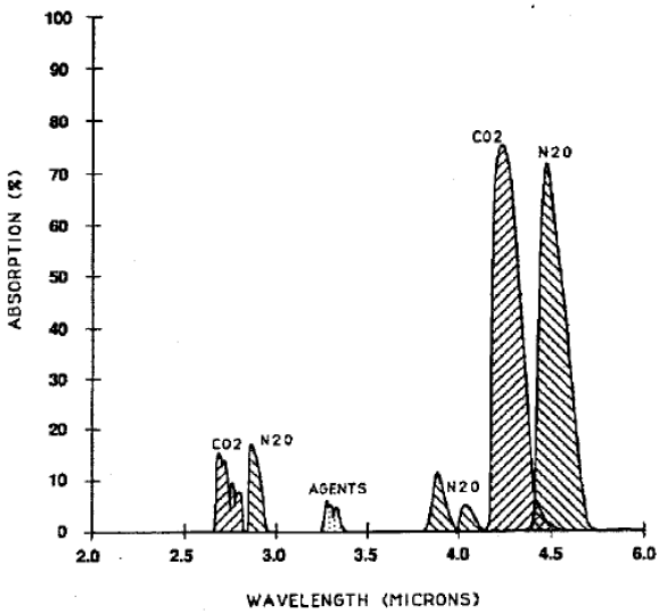

Figure 4: Infrared absorption spectrum in the range of 2-5 μm. [2] It can be seen that the absorption band of CO2 peaks between 4.2 and 4.6 μm. N_2O and water vapor (marked as H_2O in the plot) have an absorption band in the same region. These gases lead to collision broadening, resulting in erroneous CO_2 measurements. This can be avoided by addition of suitable filters in the circuitry.

where I_o and I are the incident and emergent IR light intensities; μ is the absorption coefficient of CO_2, C represents CO_2 concentration, and L is the CO_2 layer thickness. Thus, if the intensity of the light coming out of the measurement system is measured by an appropriate sensor, then the concentration of CO_2 can be determined using Equation (1).

1.1.3 LoFlo Sidestream Capnometer

This section details the construction and components of the Respironics LoFlo sidestream capnometer that was used in the project. However, the overall layout is similar for most sidestream capnometers. The details discussed in the section are from the White papers released by Respironics. [3, 4, 5, 6, 7] The three main parts of the capnometer include the sampling system, the IR gas detection and measurement system, and the pneumatics. The CO_2 gas from the nasal cannula of the patient flows through a sampling set into an IR bench consisting of a source and detector of IR radiation and then into a pneumatic system, before exiting through an exhaust port. [3] Figure 5 shows the individual components.

The LoFlo sidestream sample set consists of an interface to the patient or the breathing circuit, sampling tubing, a filter, and a sample cell. The sample set provides the complete sampling path from the patient's airway to the sample cell. The sample gas is collected from the breathing circuit through the sampling tube and directed into the measurement chamber. The dehumidification filter and the filter right before the sample cell trap the moisture in the exhaled air. [4] The sample cell is designed to permit easy connection and disconnection with a sample cell receptacle. [4] The receptacle facilitates

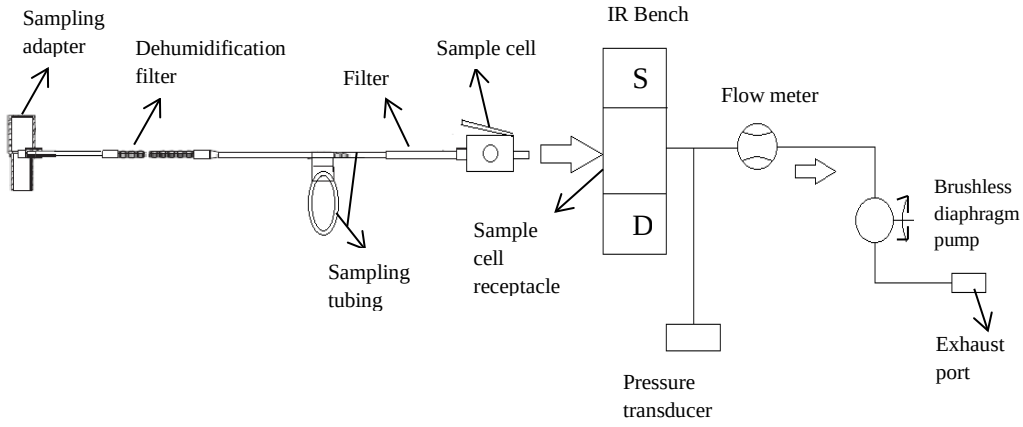

Figure 5: Schematic of LoFlo sidestream Capnometer. [3] All the components of the system– the sampling system, detachable sample cell, the IR bench with the source (S) and detector (D) of IR, the pneumatic system consisting of pressure transducer, flow meter, sampling pump, and the exhaust port- are shown. The sampling gas flows through the system in the same sequence.

proper alignment of the sample cell with the measurement optics and the pneumatics. [1]

The IR bench includes a source of IR radiation, sample cell through which the exhaled air is passed, an optical or gas filter, and a detector. [5] The wavelength of the IR source matches with the absorption band of CO_2. The IR light is focused by a lens and transmitted across the sample cell after it has been placed in the receptacle. CO_2 flowing through the sample cell absorbs some of this light at 4.26 μm. The remaining IR radiation is then passed through a filter, set at 4.26 μm to remove undesirable gases, onto a detector, and is measured. [5] This corresponds to the emergent light intensity in Equation (1), which is then used to find CO_2 concentration.

From the IR bench, the gas enters the pneumatic system. The pneumatics consists of a pressure transducer, a flow meter, and a brushless motor diaphragm pump. [5] The pressure transducer measures the circuit pressure immediately after the sample cell. A fixed orifice flow meter uses the differential pressure drop across the orifice to calculate sampling flow through the system. [6] The output of the flow meter is used to adjust the rate of sampling. A DC motor-driven diaphragm-type pump is used to draw sample through the system. [7] The sample cell receptacle contains a photo detector that detects the presence of the sample cell, to turn on the sampling pump accordingly.

1.1.3.1 Sampling pressure and flow signals. The sampling pressure and sampling flow signals are obtained from the pressure transducer and flow meter present in the pneumatic system of the sidestream capnometer.

The measured sampling pressure is the nasal respiratory pressure, measured after a constant pressure drop across the sampling tubing. It was used in the project in place of the nasal pressure signal. It represents changes in pressure as measured by the pressure

transducer during breathing. During inspiration, the lungs expand, causing a drop in pressure relative to atmospheric pressure. During expiration, the lung volume decreases. This causes pressure in the lungs to become positive with respect to atmospheric pressure. This is illustrated in Figure 6. For comparison, the measured sampling pressure during a single breath is shown along with the corresponding capnogram in Figure 7. Both the signals were recorded from the LoFlo system with the supplemental gas turned off. It can be seen that the pressure starts to rise at the beginning of expiration and continues to remain positive until the beginning of inspiration, when it starts to fall. This conformity with respiratory pressure confirms that sampling pressure can be used to identify breaths. The signal is sampled at 100 Hz.

A differential pressure flow sensor is used in the LoFlo capnometer. It incorporates a fixed orifice that generates a pressure difference across the sensor. The measured differential pressure varies as the square of flow, which can be described by Equation (2) as shown below – [6]

$$\text{Flow (mL/min)} = \frac{P_m\, T_{std}}{P_{std}\, T_m} K \sqrt{\Delta P} \qquad (2)$$

where P_m, P_{std}, T_m, and T_{std} are the measured and standard pressures (in mmHg) and temperatures (in °K), respectively, K is a correction factor that includes gas composition and other factors, and ΔP is the differential pressure (in mmHg). The P and T terms in the equation are used to convert the measured values into standard units. [6] The output of the flow meter is in Volts and it is converted to the standard units of mL/minute through the

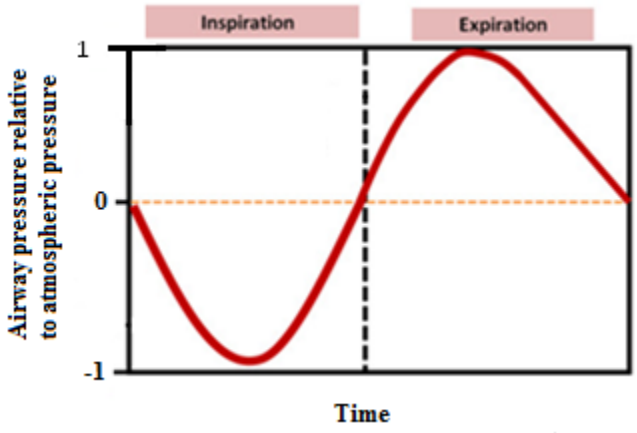

Figure 6: Airway pressure during a breathing cycle. The airway pressure recorded during inspiration and expiration is shown. The change in airway pressure is relative to the atmospheric pressure. It decreases below atmospheric pressure during inspiration and increases during expiration, facilitating the movement of air in the appropriate direction.

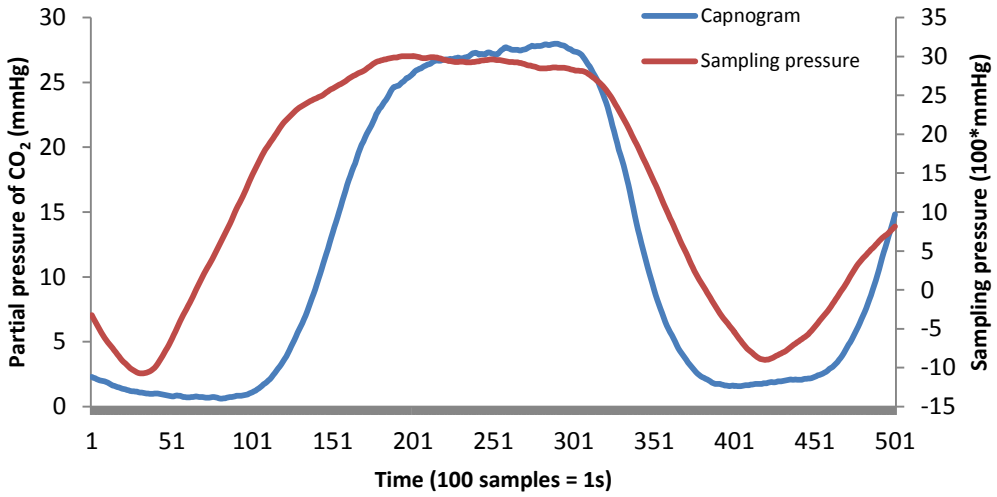

Figure 7: Capnogram and sampling pressure signals during a breathing cycle. The figure shows how the signals behave during inspiration and expiration. Both signals rise during expiration and decrease in value during inspiration. The sampling pressure signal starts to increase before the capnogram, since the partial pressure of CO_2 does not rise until the dead space is cleared.

calibration equation described by Equation (3)-

$$\text{Flow (in mL/min)} = 31.432 * \text{Flow (in Volts)} + 1.1483 \quad (3)$$

The pump regulates the sampling flow through feedback control, to help maintain a constant flow rate throughout the duration of measurement. Sample is drawn into the LoFlo at flow rates ranging from 50±10 mL/minute. The measured differential pressure is the control variable for the pump. If ΔP increases, the duration of voltage supplied to the DC motor driving the pump is reduced through pulse width modulation (PWM) so that the pump draws lesser sample per unit time, and vice versa. The sampling tube has a small diameter and hence, the gas follows a laminar flow. When the flow is laminar, ΔP depends on the viscosity of the gas, besides a few other constant factors. As the viscosity of the gas increases, ΔP increases proportionately along with a corresponding increase in the flow. To counteract this increase in sampling flow, the pump draws lesser sample through PWM and the flow is brought to baseline again.

Figure 8 depicts the filtered flow signal as measured through 10 seconds. The signal is sampled at 100 Hz. The frequency of the flow signal depends on the speed of the pump. The data logging software provides the option to choose between three pump speeds- 50 units, 80 units, or automatic pump speed setting. Using the frequency of the flow signals in each of these pump speeds, it was found that flow calculations are made approximately every 2 seconds per unit of pump speed.

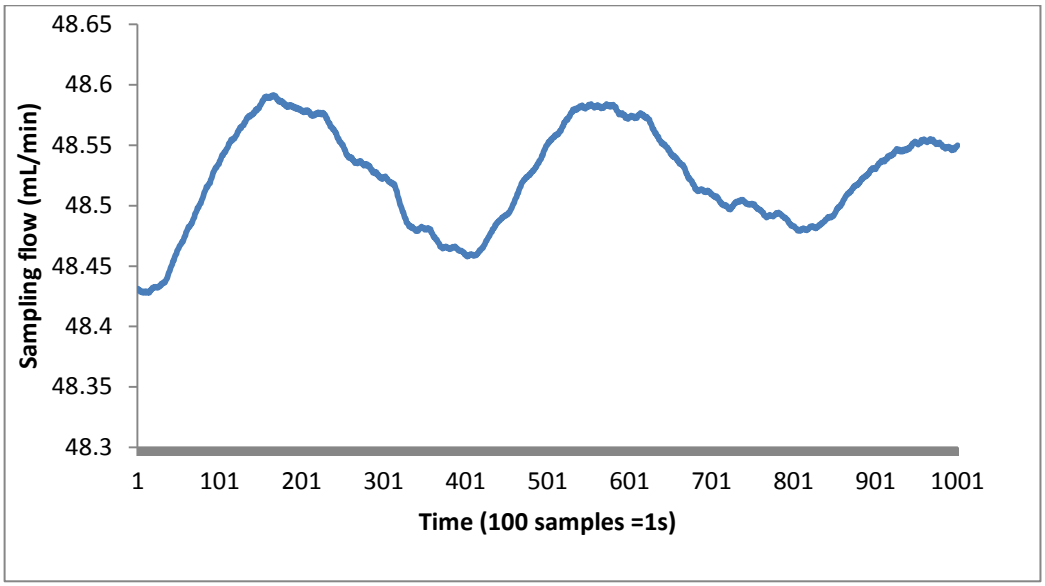

Figure 8: Sampling flow signal recorded for 10 seconds. Shown is the filtered sampling flow signal with the pump speed set to auto. Fluctuations are observed due to the changing properties of the gas being sampled. However, it should be noted that the pump succeeds in restoring the flow to its original value after every deviation.

1.2 Need for the Project

In 1999, the American Society of Anesthesiologists issued "Standards for Basic Anesthetic Monitoring", defining the role of capnography for patients receiving general anesthesia as follows-

Every patient receiving general anesthesia shall have the adequacy of ventilation continually evaluated. Continual monitoring for the presence of expired carbon dioxide shall be performed unless invalidated by the nature of the patient, procedure or equipment. Continual end-tidal carbon dioxide analysis, in use from the time of endotracheal tube/laryngeal mask placement, until extubation/removal or initiating transfer to a postoperative care location, shall be performed using a quantitative method such as capnography, capnometry or mass spectroscopy.[a]

It has also been shown in a study that 74% of ICU airway deaths could have been prevented if continuous capnography had been used. [8]

Despite the proven value of capnography, it has been shown in studies that its percentage of false alarms is no better than previous methods of monitoring ventilation. [9, 10, 11, 12, 13, 14, 15] Falsely low etCO_2 values often arise due to errors in sampling of the gas. Mixing of the CO_2 gas with supplemental O_2 or sampling CO_2 from the nasal cavity in mouth breathing patients significantly reduces the size of the capnogram and makes the system detect apnea. [16] At slow respiratory rates, it is common to see ripples on the plateau and descending limb of the capnogram. See Figure 9. These are called cardiogenic oscillations and arise from gas movements created by pulsations of the aorta and heart. This is represented in Figure 10. The ripples may be misconstrued as separate breaths, [18] leading to failure to detect apnea.

[a] American Society of Anesthesiologists. Standards of the American Society of Anesthesiologists: Standards for Basic Anesthetic Monitoring. Available at: https://www.asahq.org/For-Members/~/media/For%20Members/documents/Standards%20Guidelines%20Stmts/Basic%20Anesthetic%20Monitoring%202011.ashx. Accessed August 13, 2014.

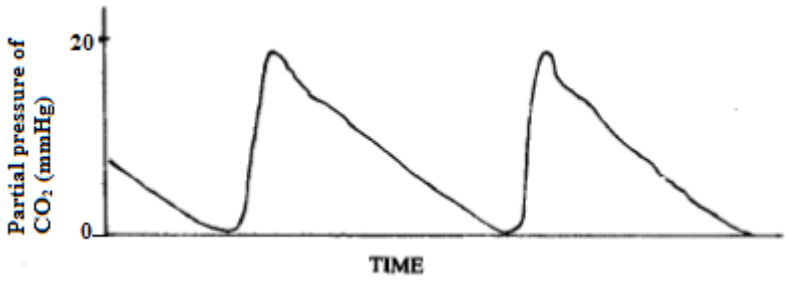

Figure 9: Capnogram recorded during delivery of supplemental gas. [17] The supplemental gas dilutes CO_2 and interferes with the measurement system, resulting in the projection of a falsely low etCO_2

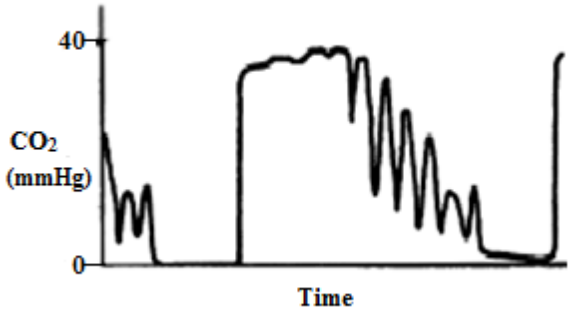

[b]

Figure 10: Capnogram recorded during cardiogenic oscillations. Cardiogenic oscillations, seen as ripples on the displayed capnogram, occur during slow breathing as a result of the anatomical proximity of the heart and lungs. They are synchronous with cardiac contractions and are visible during the final phase of expiration and beginning of inspiration

[b] http://web.squ.edu.om/medLib/MED_CD/E_CDs/anesthesia/site/content/v03/030383r00.htm. Accessed March 16, 2014.

Detection of apnea using respiratory pressure was first described by Guyatt et al.[19] Since then, the nasal pressure signal has proven to be accurate even during nasal obstruction, compared to face-mask pneumotachography, the gold standard of monitoring respiration during sleep, [20] and better at describing respiratory status than a thermistor or thoraco-abdominal bands during sleep studies. [1] Having established its superiority over a few conventional respiratory monitoring methods, it would be worthwhile to compare the performance of the pressure signal with the capnogram and see if it can provide more reliable results in situations where the latter fails.

1.3 Literature Survey

This section focusses on the work done using the nasal pressure signal and the performance of the signal. In all the studies discussed below, the pressure signal was derived from a standard nasal cannula connected to a pressure transducer.

Nasal pressure began to be used in medical studies as a way of quantifying respiratory status during sleep. [21] It was used to determine the respiratory flow signal and the two signals together were used to detect breaths and abnormal respiratory events. In one of the earliest studies, it was used in patients with sleep apnea-hypopnea syndrome (SAHS). [15] Its performance was compared with the conventional sleep respiration assessment using thermistors and thoraco-abdominal bands. The authors determined that nasal pressure, thermistors, and bands detected 96.8%, 60%, and 83% of true respiratory events, respectively, with a sensitivity of 96%, 62%, and 81%, respectively.

Additionally, it was found to have a better dynamic response than the other two methods. Unlike the conventional methods, partial nasal obstructions did not affect the

performance of the nasal pressure-based breath detection technique. Crowley et al. compared the performance of the nasal pressure signal and standard polysomnography for assessment of sleep apnea using apnea-hypopnea index. [23] A strong correlation of 86% was observed between the methods in the lab, with the nasal pressure signal having a sensitivity and specificity of 100% and 92%, respectively. It identified all the true negative cases correctly, thus reducing the number of false alarms. A sensitivity of 67% was obtained for severe sleep apnea which was attributed to the small size of the test population.

Hosselet et al. established that nasal pressure and the corresponding inspiratory flow could be used to confirm flow limitations and help diagnose upper airway resistance syndrome (UARS). [24] Resistance was determined using peak inspiratory flow and pressure and it was increased for breaths with a flattened flow contour. This criterion separated the 10 symptomatic subjects from the 4 nonsymptomatic subjects with an accuracy of 100%. In making a case for using nasal pressure as a noninvasive method for detecting respiratory effort related arousals (a reduction in respiratory gas flow and increased resistance associated with arousal), Ayappa et al. concluded that it produced the same results as the standard, invasive technique of esophageal manometry, but had a 11% increased sensitivity. [25]

The nasal pressure signal was also credited for detecting events undetected by thermistors, such as obstructions and mouth-breathing, thereby increasing the accuracy of breath monitoring. [26, 27, 28] Complete oral breathing could be a disadvantage, since it appeared as apnea on the pressure signal. [26] A number of studies concluded that the pressure signal had more sensitivity to detecting breaths than thermistors. [26, 27, 28, 29]

I could not find work on the usefulness of the nasal pressure signal on sedated subjects and its performance compared to the capnogram. However, a consistent result through the work discussed above is the high accuracy and sensitivity of the pressure signal in respiratory monitoring and its capability to successfully detect breaths even during events of flow limitations, partial nasal obstructions, and partial mouth breathing. These conditions are known to be detrimental to the quality of the capnogram and are most likely to be inferred as apneic events by the capnogram. They cause a drop in the etCO_2 value and an overall reduction in the size of the signal, much like the presence of supplemental O_2. Having proven its worth in similar situations, there is a possibility that the pressure signal might work well in the presence of supplemental O_2, reduce the false negative percentage, and increase the accuracy and reliability of breath detection.

CHAPTER 2

BENCH TESTING

2.1 Testing the Utility of the Sampling Pressure Signal

It was established in Chapter 1 that the sampling pressure signal can be used to detect breaths. As a preliminary way of estimating the accuracy of the signal relative to the capnogram, breath time and the average breath rate was calculated from both the signals when supplemental gas was not given and the results were compared. However, the pressure and CO_2 signals are not aligned in time. The remote CO_2 sensor location results in a long transport between the sampling site and the sensor, causing a total response delay time in the capnogram. Instead of an instantaneous upswing in the CO_2, a rise time of about 200 ms can be observed. This delay is shown in Figure 11. However, the sampling pressure and sampling flow signals are instantaneous. So the sampling pressure signal had to be delayed with respect to the CO_2 signal so that the breaths from both the signals were correlated and a useful comparison could be made. The alignment between the signals is shown in Figure 12.

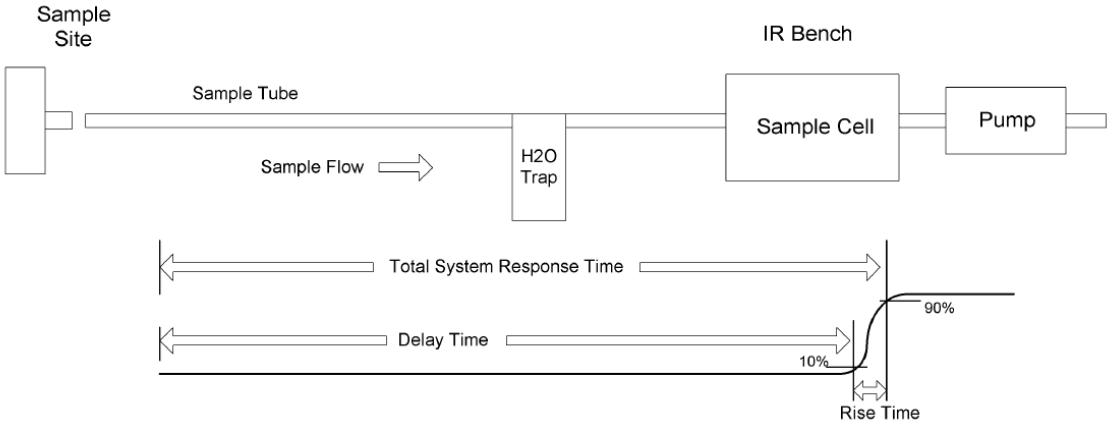

Figure 11: Delay associated with the capnogram. [17] The inherent delay between the time of sampling and measurement in a sidestream capnometer results in a delay in the display of the capnogram and a rise time delay of about 200 ms.

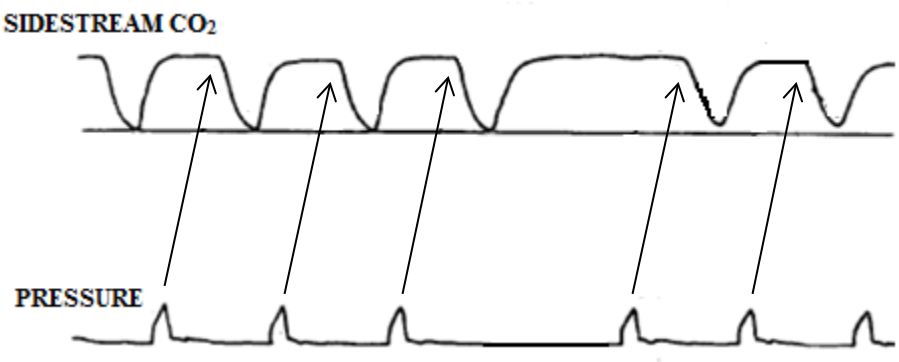

Figure 12: Time relationship between the CO_2 and pressure signals. [17] The figure shows the delay in the sidestream CO_2 signal compared to the instantaneous pressure signal, making alignment of the signals a necessity for useful comparison.

2.1.1 Signal Alignment

2.1.1.1 Inspiratory phase alignment. During expiration, the pressure signal peaks instantaneously. The capnogram, however, does not rise until the dead space is cleared and CO_2 from the alveoli is expired. On the other hand, both signals start to drop at the beginning of inspiration. The start of inspiration is represented by the etCO_2 point on the capnogram and the positive peak on the pressure signal. Hence, matching these points on every breath from the two signals would automatically align both the signals completely. A simple and effective way of detecting these points is to take the first order differential of the signals, which would be zero or negative throughout inspiration. Hence, the positive part of the differential is discarded and the rest is stored in a new variable. The pressure signal was delayed between -1000 samples and 1000 samples (approximately two breaths) in increments of 1. The goal was to determine by how many samples the pressure signal had to be shifted so that the start of inspiration in both the signals was aligned. The differential of the capnogram and each delayed version of the pressure signal were multiplied. The highest product corresponds to the best possible alignment. The delay corresponding to the maximal product was applied to the pressure signal to align it with the capnogram. The coefficient of determination (R^2) was calculated between the capnogram and all the shifted versions of the pressure signal. R^2 would be maximal when the two signals are best aligned. Five-minute breathing files were collected from 6 spontaneously breathing volunteers and used in analysis. The algorithm is depicted in Figure 13.

The results from the algorithm indicated that the pressure signal had to be delayed by 505 ± 13 samples to be aligned with the CO_2 signal. The product of differentials

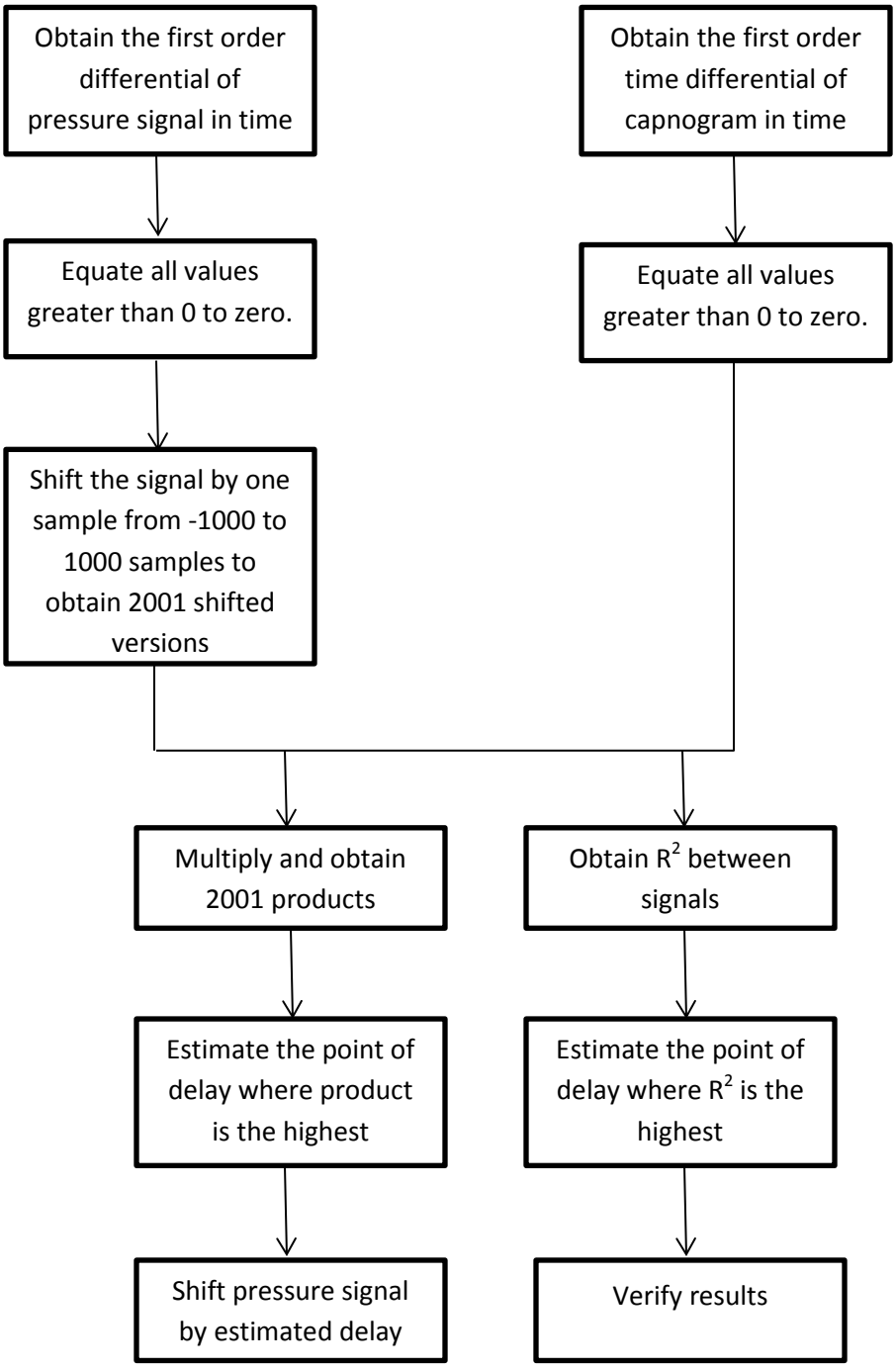

Figure 13: Flow chart of inspiratory phase alignment algorithm. The flow chart explains the various steps involved in aligning the sampling pressure and CO_2 signals. This method aligns the distinct points in the signals representing the start of inspiration

obtained over the range of delays and the aligned signals for Subject-1 are shown in Figure 14. The R^2 at the best delay as obtained by the algorithm was 63 ± 19% of the maximal R^2 obtained between the signals. Refer to Figure 15 for the location of the maximal R^2 and the best delay obtained for Subject-1 from the algorithm.

Though the individual breaths were aligned quite well, the inspiratory and expiratory phases of each breath were not aligned in time. If the algorithm is accurate, the location of the peak R^2 value would coincide with the delay obtained by the algorithm. However, this was not observed in any of the data files aligned by this method.

2.1.1.2 Least squares alignment. When the normalized pressure and CO_2 signals are aligned in time, the error or difference between them is minimal. The second algorithm is based on this concept and is represented as a flow chart in Figure 16. The pressure signal was shifted over the same range of delays as before, between -1000 samples and 1000 samples in increments of 1. The sum of square of differences between the CO_2 signal and each shifted version of the pressure signal was obtained. The delay corresponding to the least sum (or least error) was applied to the pressure signal to align it with the capnogram. R^2 was determined between the capnogram and the pressure signal shifted over the entire range of delays.

The delay required for the best possible alignment between the signals was determined by the algorithm as 549 ± 14 samples. See Figures 17 and 18 for the results obtained for Subject-1. It was found that the R^2 value was maximal when the pressure signal was delayed as determined by the algorithm in all the data files.

This method yields better correlation between the aligned signals than the previous algorithm and was chosen for future analysis. It should be noted that this

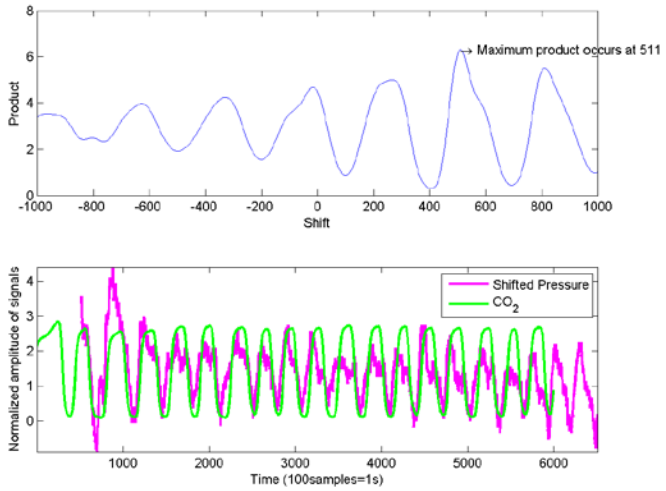

Figure 14: Alignment based on start of inspiration. The upper plot shows that the product between the time derivative of the shifted pressure signal and CO_2 signal is maximal when the pressure signal is shifted by 511 samples. The signals look as shown in the bottom plot after applying the obtained delay to the pressure signal. It can be seen that individual breath from both signals are aligned well. Inspiration and expiration in each breath are not matched well enough.

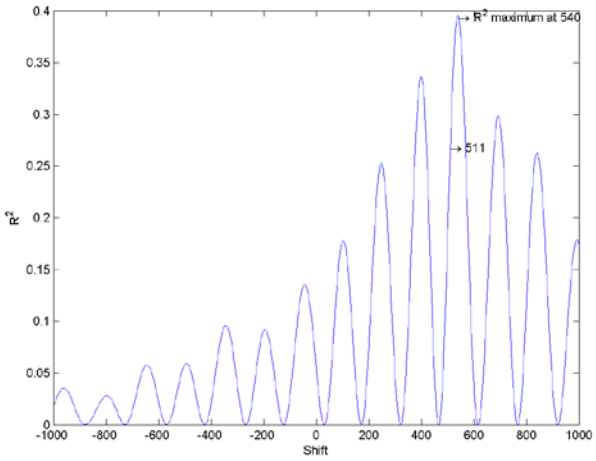

Figure 15: Correlation between sampling pressure and CO_2 signals. The coefficient of determination, R^2, is obtained between the shifted pressure signal and the CO_2 signal. The maximal R^2 was obtained when the pressure signal was shifted by 540 samples while the algorithm determined the best delay for the pressure signal as 511 samples. An agreement between these values indicates high performance of the algorithm.

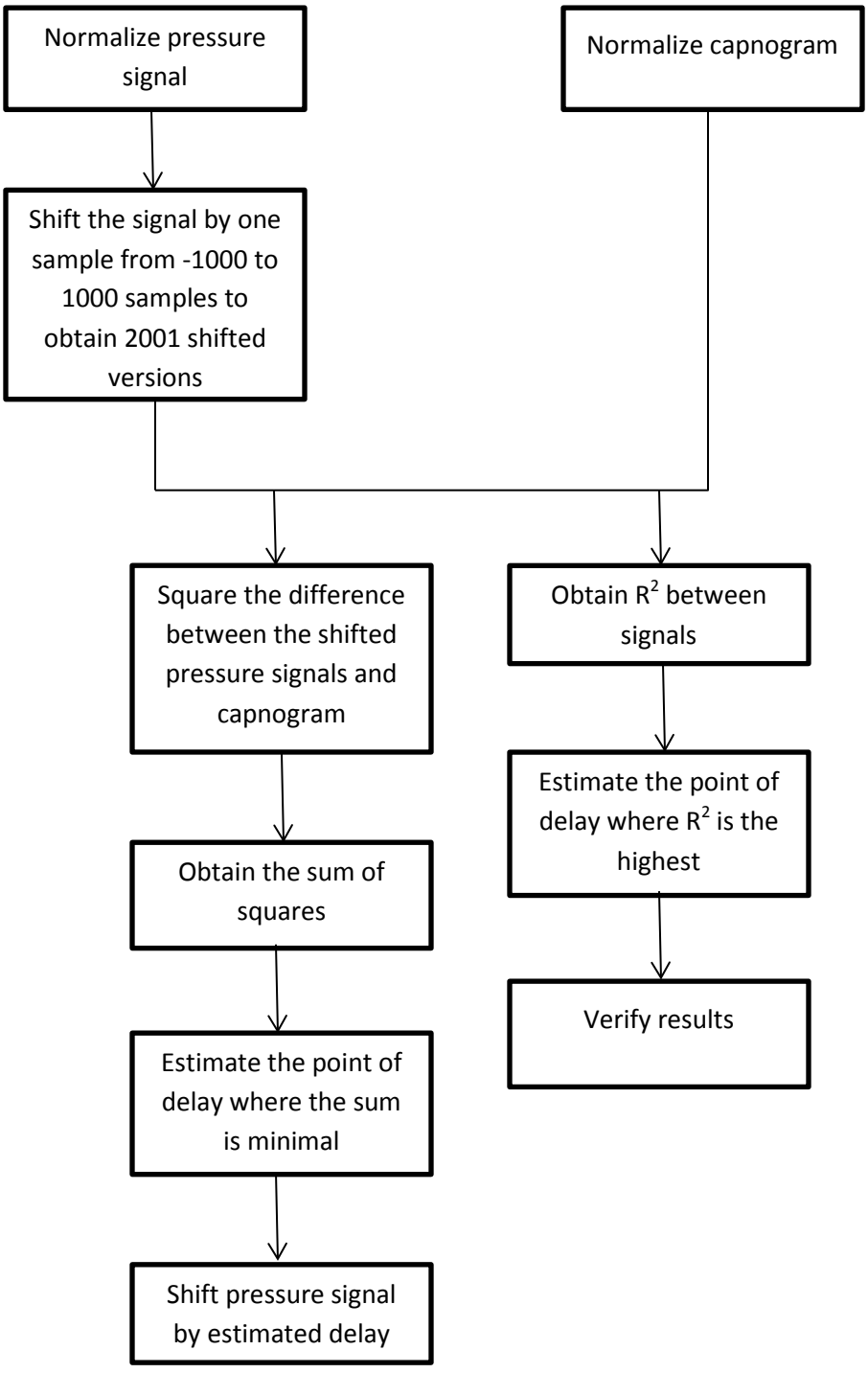

Figure16: Flow chart of least squares alignment algorithm. This algorithm aligns the sampling pressure and CO_2 signals based on the sum of square of differences between the signals.

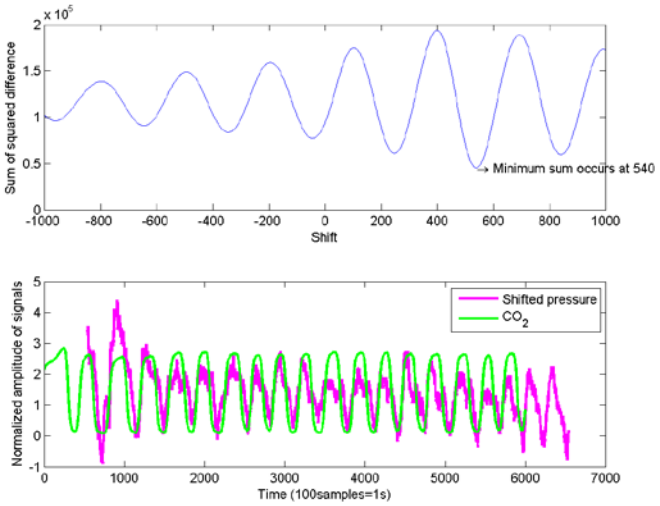

Figure 17: Alignment based on least squares technique. The sum of least squares obtained for each position of the pressure signal is shown in the top plot. The least sum, corresponding to least error, was obtained at 540 samples. This delay was applied to the pressure signal. The signals aligned in this manner are shown in the bottom plot. Breaths from both signals are aligned in time. However, individual respiratory events in each breath do not coincide.

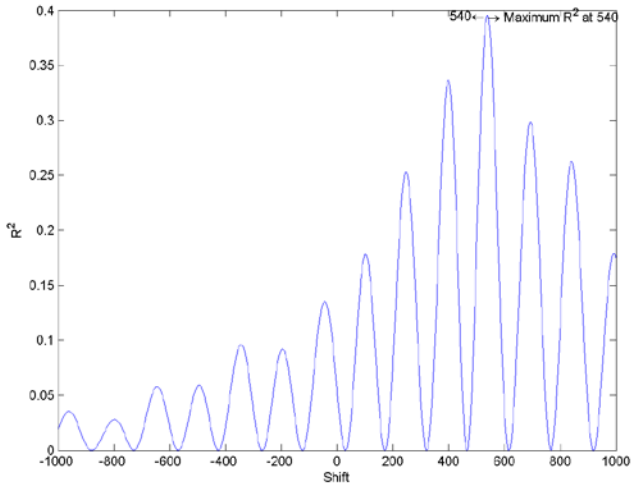

Figure18: Correlation between sampling pressure and CO_2 signals. The coefficient of determination, R^2, was obtained between the shifted pressure signal and the CO_2 signal. The maximal R^2 was obtained when the pressure signal was shifted by 540 samples. This coincided with the delay obtained by the algorithm, confirming the accuracy of the alignment technique.

algorithm, like the previous one, also aligns only individual breaths and not the individual inspiratory and expiratory events in each breath. When the entire pressure signal is shifted by a specific number of samples as dictated by any algorithm, exact alignment of each breath is very difficult to achieve, owing to the differences in the morphology of the signals.

2.1.2 Estimation of Breath Rate

The aligned signals were used to calculate individual breath times and average breath rate for the same set of six volunteer files. The average amplitude of the individual signals was set as its corresponding threshold. The duration when the signal was higher in value than the threshold was defined as the ON period. The OFF period was defined as the duration when the signal was lower in value than its corresponding threshold. The sum of one OFF period and one ON period was defined as a breath time. The maximal and minimal breath times obtained from both signals were displayed along with the average breath time and breath rate. The correlation coefficient was determined between the individual breath times obtained from the two signals. These steps are depicted in the form of a flow chart in Figure 19.

2.1.2.1 Results. The correlation between breath times estimated from the two signals for the six data files was found to 0.70 ± 0.18. Strong agreement between the parameters obtained from the pressure signal and the reference capnogram establishes the usefulness and accuracy of the sampling pressure signal. The parameters obtained for Subject-1 are depicted in Table 1. The individual breath times obtained from both signals are plotted against one another in Figure 20 to show correlation.

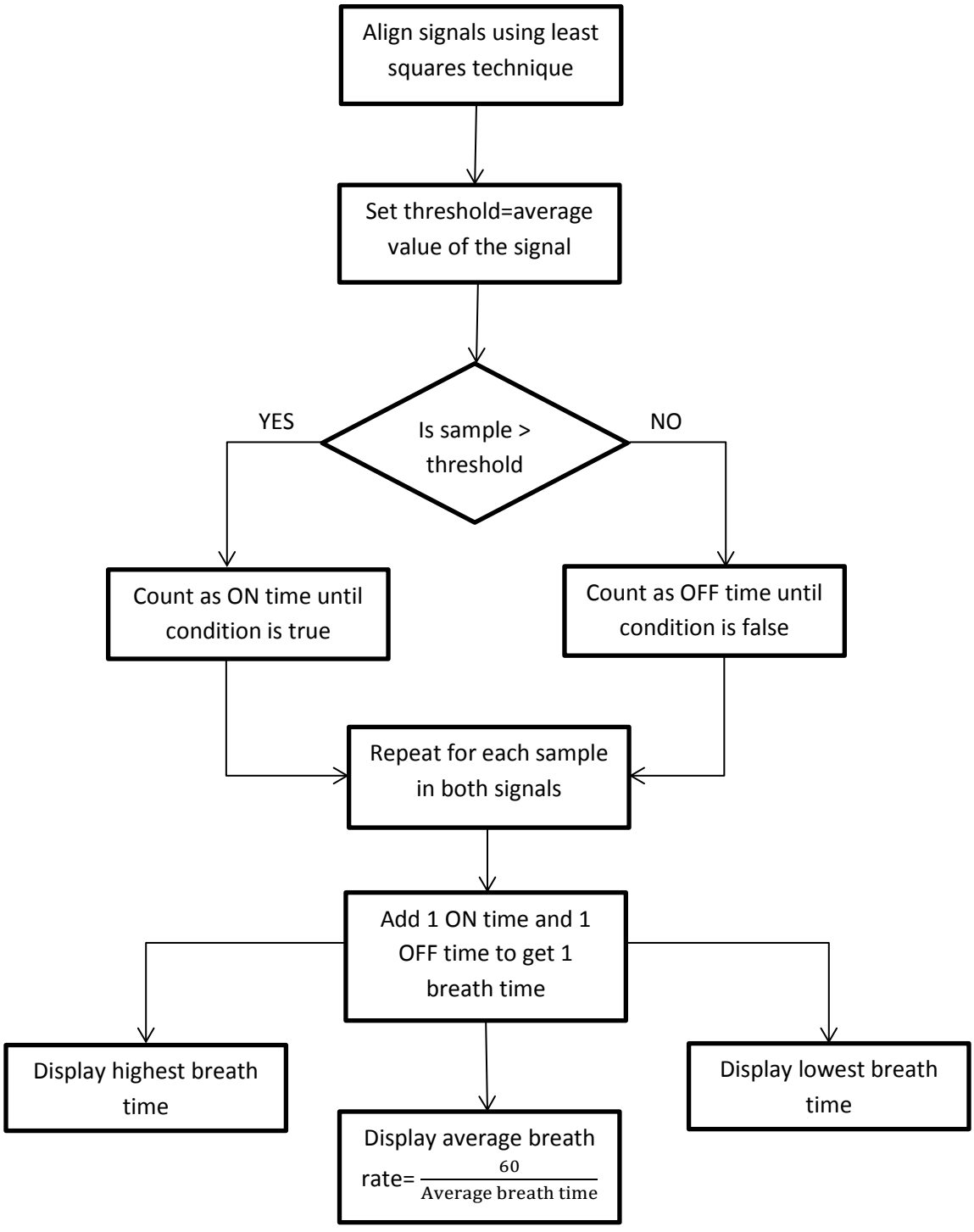

Figure 19: Flow chart of breath rate estimation algorithm. The steps in obtaining the average breath rate, and average, lowest and highest breath times from both signals are depicted.

Table 1.Respiratory parameters obtained for Subject-1 after aligning the CO_2 and pressure signals.

Parameter	From CO_2	From pressure
Average breath time	2.00 ± 0.17 s	2.96 ± 0.44 s
Minimal breath time	1.25 s	1.04 s
Maximal breath time	4.43 s	4.18 s
Breath rate	20.09 /minute	20.27 /minute

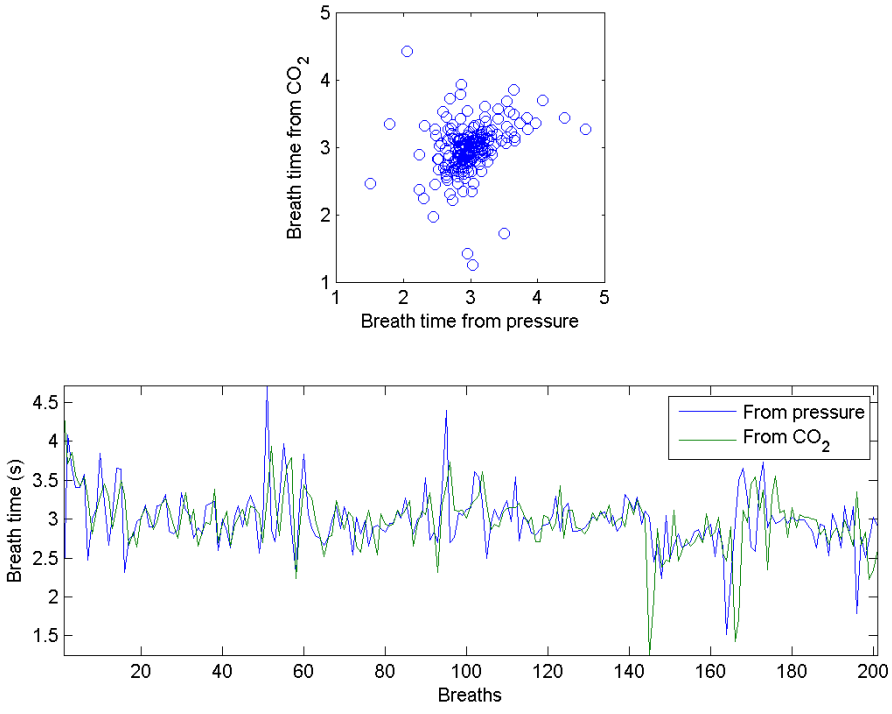

Figure 20: Comparison of breath times. The breath times obtained from the CO_2 signal and pressure signal are plotted against each other in the top plot. A 45° line indicates perfect correlation between the axes. The bottom plot indicates the actual breath times obtained from the signals for each breath recorded during the period of study.

2.2 Bench Data Collection

The next step was to examine the behavior of the capnogram, the sampling pressure, and the sampling flow signals in the presence of supplemental gases. A bench experiment was set up to simulate washout of CO_2 by O_2 or air to visualize the effects the gases had on the signals, before clinical data could be collected from human volunteers. The set-up was as follows. CO_2 was infused into one side of a two chamber mechanical lung that was connected to a manikin head. The other side of the test lung was mechanically ventilated using a Siemens 900C ventilator. A physical connection between the chambers enabled simulation of spontaneous breathing in the nonventilated lung. The LoFlo cannula was placed in the nostrils of the manikin with air or O_2 added into one nostril at 0.5 LPM, 2.0 LPM, and 5.0 LPM of flow. The LoFlo system drew sample from the other nostril. The minute ventilation was set to 6 LPM with a rate of 8 breaths per minute (bpm), 12 bpm, or 20 bpm. The set-up is demonstrated pictorially in Figure 21.

2.2.1 Results

At all flow rates, both air and O_2 washed out CO_2 towards the end of expiration. The rate of gas flow produced a difference in the $etCO_2$ recorded with each gas. In the case of air, $etCO_2$ was 13% less at 5 LPM than at 0.5 LPM. On changing the flow rate of O_2 from 0.5 LPM to 5 LPM, the $etCO_2$ dropped by 36%. It was observed that O_2 had a more detrimental effect on the $etCO_2$ than air at all flow rates. At 0.5 LPM, 2 LPM, and 5 LPM, the observed $etCO_2$ was 13%, 15%, and 37% lesser with O_2 than with air. The signals recorded at a flow rate of 5 LPM are shown in Figure 22.

In general, the pressure signal amplitude increased with the flow rate. At 5 LPM

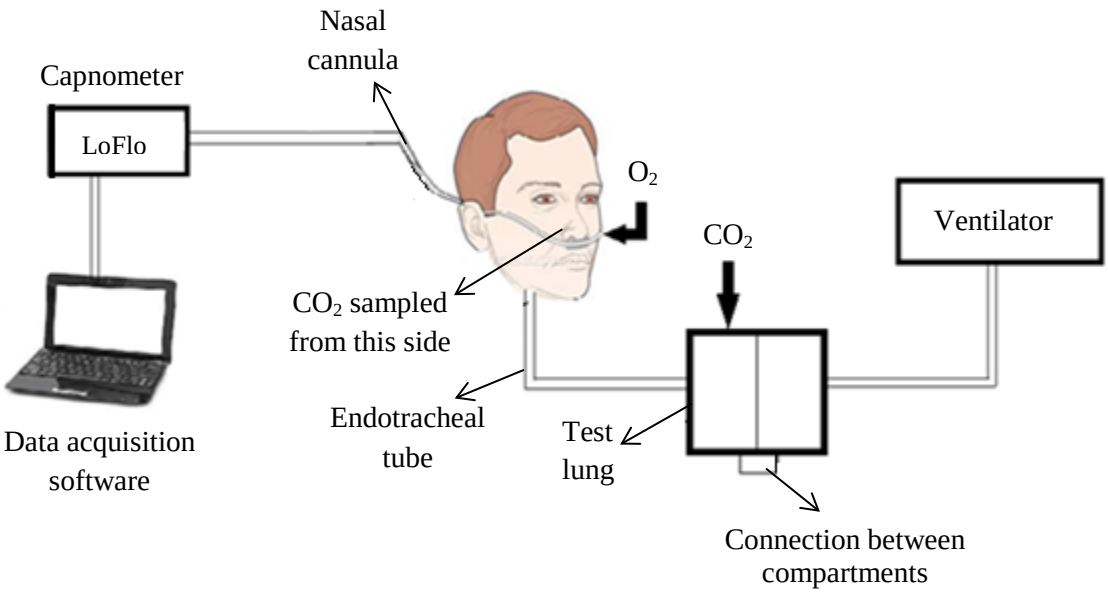

Figure 21: Bench study set-up. Shown is a schematic of the set-up used to simulate washout of CO_2 by supplemental gas. Air or O_2 was delivered at rates of 0.5 LPM, 2 LPM, and 5 LPM. CO_2, sampling pressure, and sampling flow signals were recorded and analyzed.

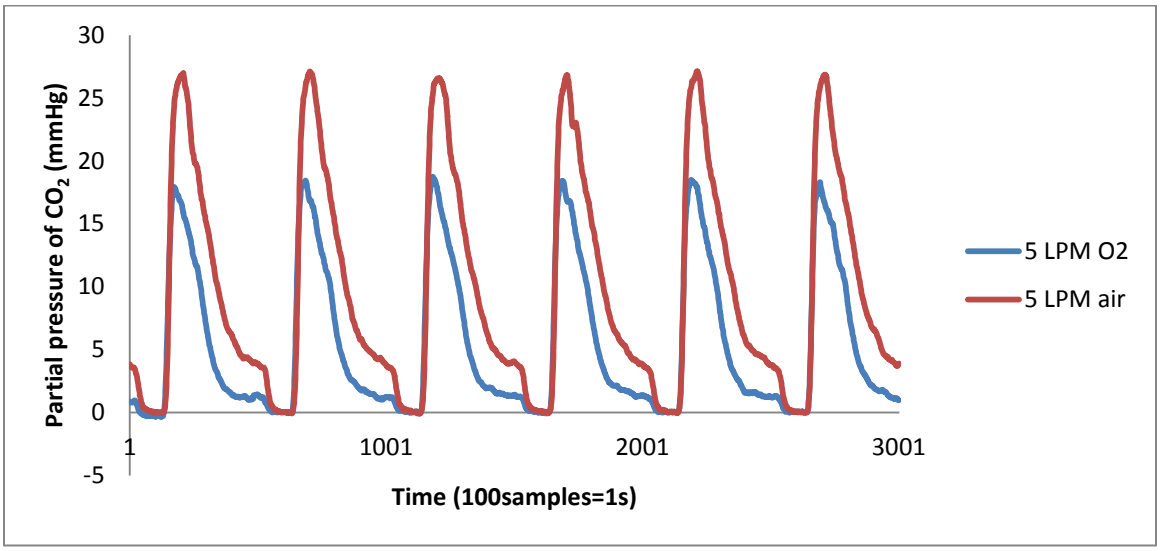

Figure 22: Capnogram recorded with 5 LPM flow rate. The CO_2 signal obtained with 5LPM of O_2 and air are shown in the figure. It is seen that the etCO_2 obtained at 5LPM of O_2 is 37% lesser than its value with 5LPM of air.

of air, the pressure signal was 7 times its size at 0.5 LPM. In the case of O_2, the amplitude increased by 44 times on changing the flow from 0.5 LPM to 5 LPM. While the recorded signals were about the same size at 0.5 LPM, it was 4.2 times and 5.6 times bigger in amplitude with 2 LPM and 5 LPM of O_2, respectively, than at the same flow rates of air. The signal looked regular in the presence of air, with distinct inspiratory, expiratory, and pause phases. When O_2 was delivered through the cannula, it looked like a distorted, triangular waveform. Another notable difference in the signal in the presence of O_2 delivered at high flow rates was the appearance of a second peak at the beginning of expiration. Refer to Figure 23.

The sampling flow signal in a LoFlo capnometer is supposed to be maintained at 50 ± 10 mL/min. This was true in the presence of air. However, when O_2 was present in the cannula, the signal showed significant swings during each breath. At 0.5 LPM, 2LPM, and 5LPM of O_2, the signal was 4.4 times, 5.7 times, and 8 times bigger in amplitude, respectively, than its amplitude in the presence of air at the same flow rates. Figure 24 depicts the signals recorded at a flow rate of 5 LPM.

All the results discussed so far were for a respiratory rate of 12 bpm. Similar trends were observed in the signals recorded at rates of 8 bpm and 20 bpm. The amplitude of the second peak observed at the beginning of expiration in the sampling pressure signal increased in amplitude with decreasing respiratory rate. The signals recorded at each respiratory rate are shown in Figure 25.

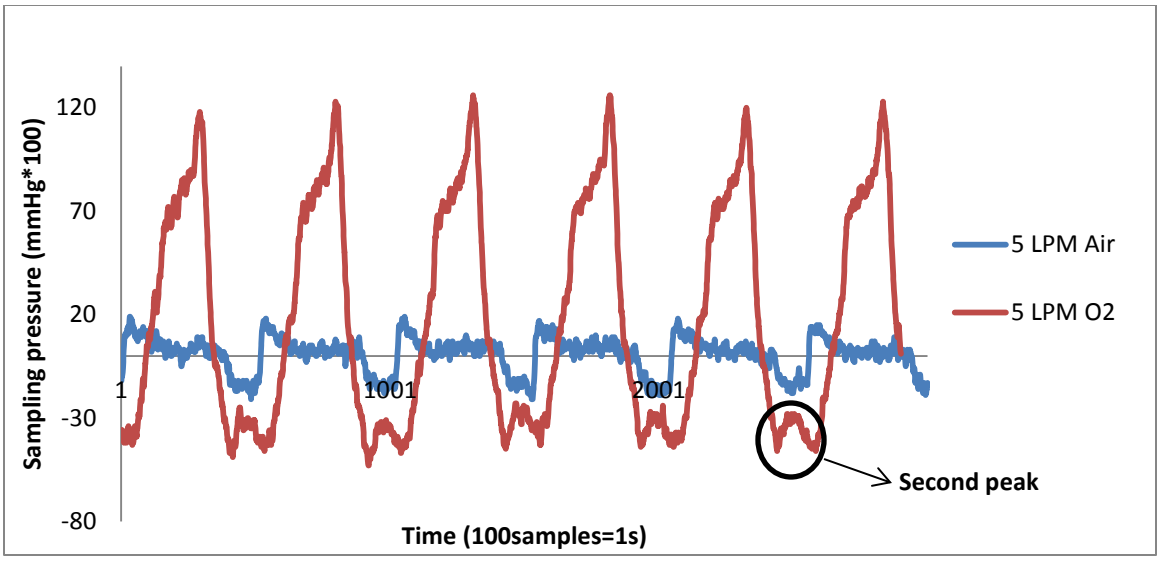

Figure 23: Pressure signals recorded at 5 LPM of supplemental gas. The pressure signal recorded with O_2 is 44 times its size with 5 LPM of air. The presence of an additional peak at the beginning of expiration is also evident in the signal recorded with O_2. This feature is not observed in the presence of air.

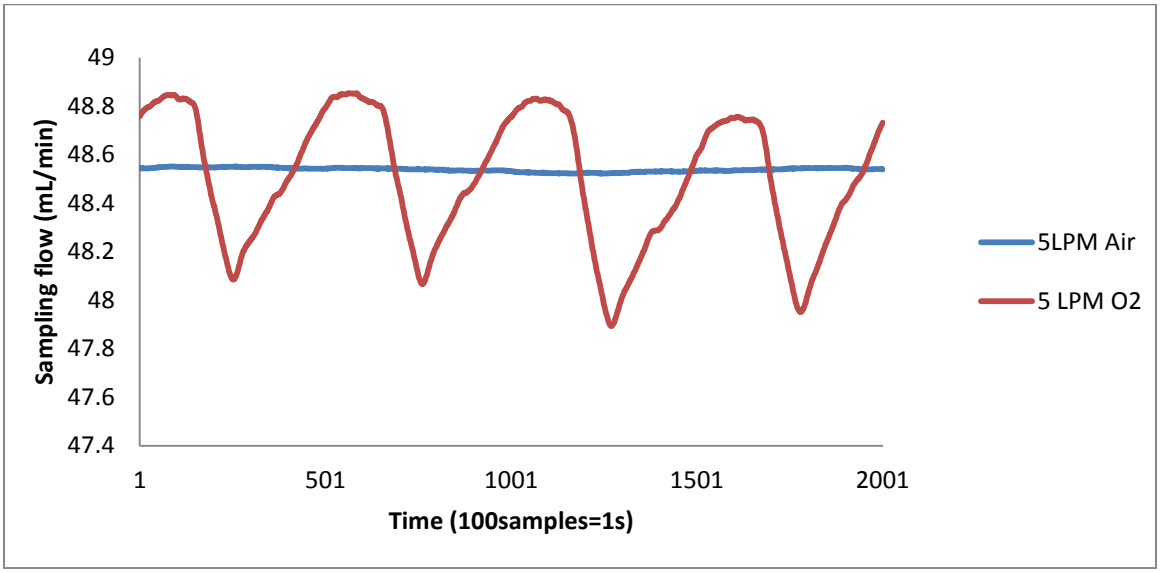

Figure 24: Sampling flow signals at 5LPM of supplemental gas. Shown above are the sampling flow signals recorded with 5LPM of air and O_2. The signal remained considerably flat in the presence of air. The introduction of O_2 in the nasal cannula caused significant swings in the signal during each breath. The amplitude of the signal with O_2 was 8 times its amplitude with air at 5 LPM.

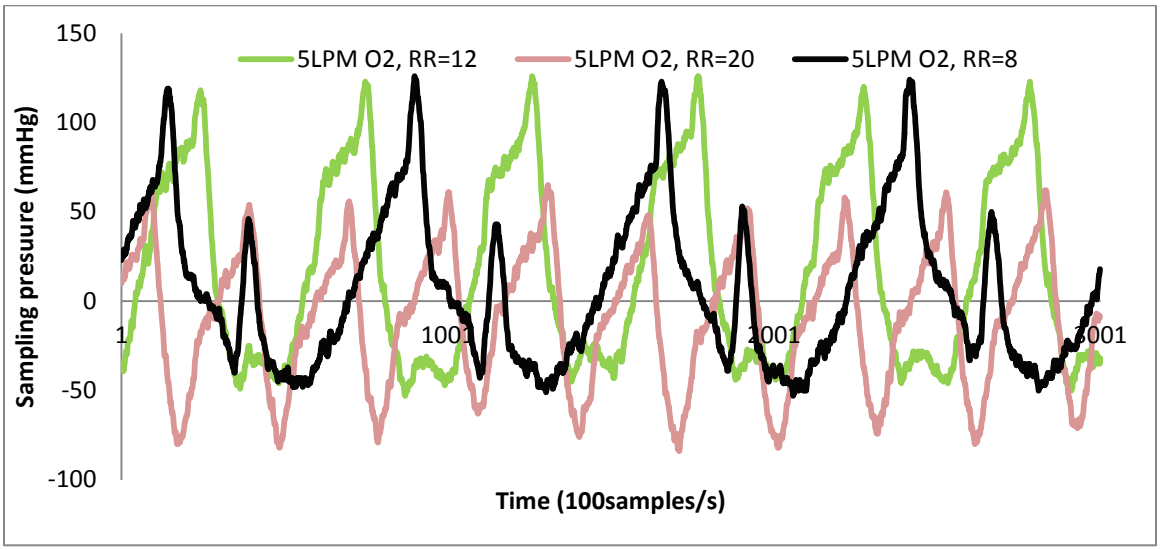

Figure 25: Pressure signals at different breath rates. The sampling pressure signals recorded at a breath rate of 8, 12, and 20 breaths per minute are shown in the plot. It is evident that the additional peak observed at the beginning of expiration increases in amplitude with decreasing breath rate.

2.2.2 Discussion

The anomalies in the signals were observed only in the presence of supplemental O_2, suggesting that the higher viscosity of O_2 might produce changes in the functioning of the pneumatic system of the capnometer. However, the manikin used in the study did not have an anatomically correct nasal/oral cavity. This might have also had an impact on the results. So the next step was to collect data from human volunteers and see if the signals reacted similarly to the presence of the supplemental gases.

2.3 Data Collection from Volunteers

The aforementioned signals were collected from 4 human subjects with air or O_2 delivered at 0.5 LPM, 2 LPM, and 5 LPM through a nasal cannula. The subjects were initially asked to breathe at a fast pace, and then at a slow pace. The signals were recorded throughout the duration of breathing.

2.3.1 Results

The capnograms, as shown in Figure 26, looked similar in the presence of air and O_2, irrespective of the rate at which they were delivered. At 0.5 LPM and 2LPM of gas flow, there was no difference in the amplitude of the sampling pressure or flow signals. At 5 LPM of O_2, the pressure signal amplitude was 1.75 times the amplitude with 5 LPM of air. This difference is demonstrated in Figure 27. Though second peaks were observed in the signal in the presence of O_2, they were not as prominent as seen with the manikin and were not seen in every breath. They were not due to rebreathing, as verified from the corresponding capnograms. The amplitude of the sampling flow with 5 LPM of O_2 was

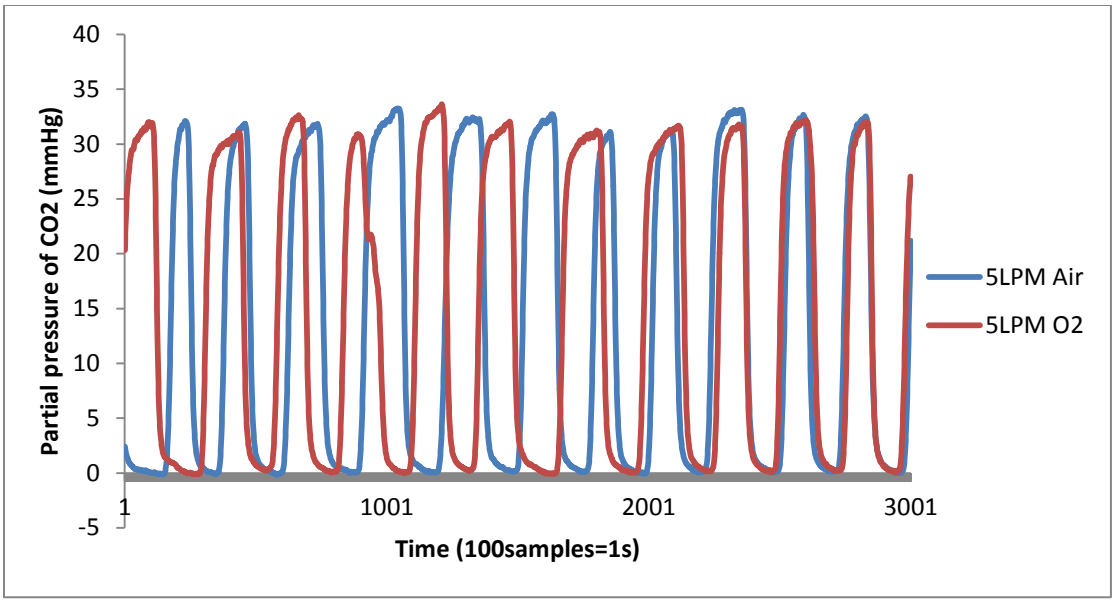

Figure 26: Capnogram recorded from human volunteer. Shown are CO_2 signals recorded from one of the volunteers in the presence of air and O_2. The signals do not show pronounced washout, irrespective of the gas, even at 5 LPM.

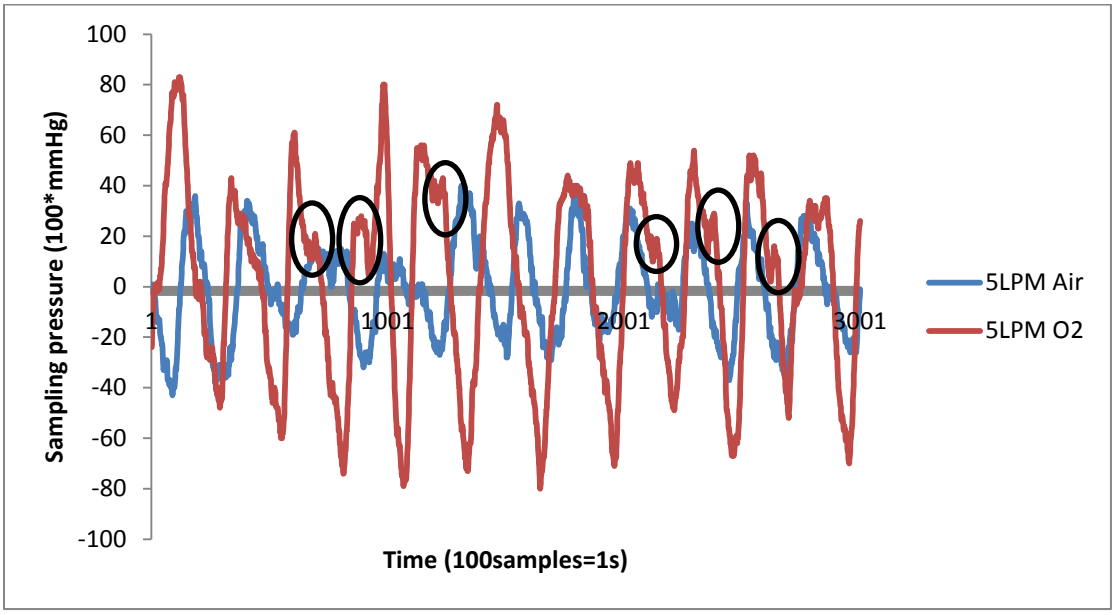

Figure 27: Sampling pressure signals recorded from human volunteer. The pressure signal is 1.75 times its size with O_2 than with air. Double peaks are visible in a few breaths when O_2 is delivered, but they are smaller in size compared to those from the manikin.

1.7 times its amplitude with 5 LPM of air as shown in Figure 28. Breath-wise fluctuations in the signal were observed at 2 LPM and 5 LPM of O_2. Figure 29 shows that the recorded pressure signal looked normal when the subject was breathing fast. However, double peaks were prevalent when the respiratory rate decreased. This can be seen in Figure 30. It was as though the increased time between breaths had a greater impact on the morphology of the signal.

2.3.2 Discussion

It can be concluded that the inaccurate construction of the nasal cavity in the manikin caused an exaggeration in the results observed in the presence of supplemental O_2. However, a few trends observed in the bench study during the delivery of supplemental O_2 were detected in the signals recorded from humans as well, namely an increase in the amplitude of the sampling pressure and the flow signals, and appearance of second peaks during expiration in the pressure signal.

The probable cause for the increase in amplitude of the signals might be the higher viscosity of supplemental O_2 compared to air. O_2 is 17% more viscous than air. Hence, during inspiration in the presence of supplemental O_2, the sampling pressure would be more negative than with air. This in turn increases the peak-to-peak amplitude of the signal. At the beginning of expiration, O_2 is the first gas to be exhaled until dead space is cleared and the capnometer can sample CO_2. This is depicted in a screen shot of the Capnomac Ultima (Datex, Helsinki, Finland) analyzer shown in Figure 31. The concentration of O_2 and CO_2 during breathing is displayed. Rise in the percentage of O_2 can be seen at the beginning of expiration. This might be the reason for the appearance of

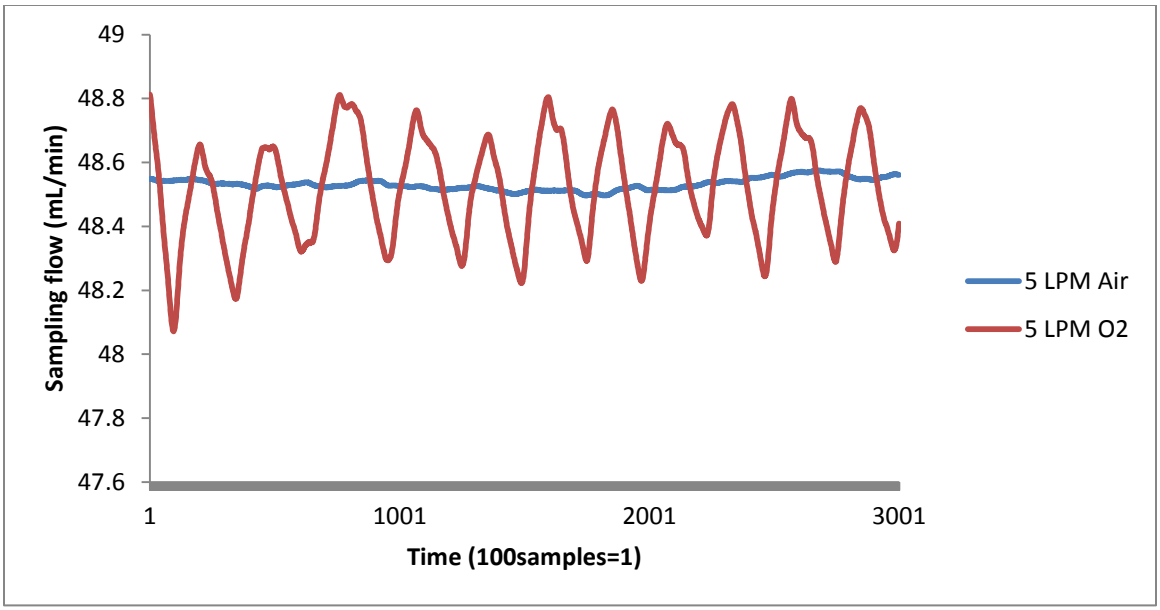

Figure 28: Sampling flow signals recorded from human volunteer. At 5LPM of O_2, the signal shows fluctuations in every breath and its amplitude is 1.7 times bigger with O_2 than with air.

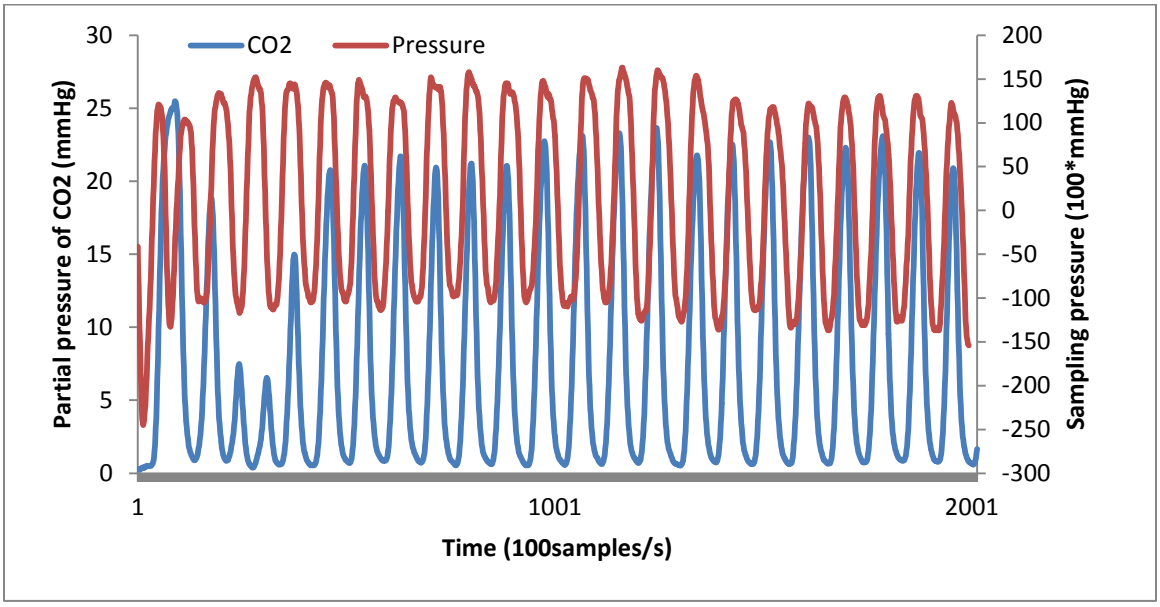

Figure 29: Signals recorded during fast breathing. The CO_2 and pressure signals recorded in the presence of 5 LPM of O_2 when the subject was taking fast breaths are shown. The pressure signal does not show double peaks and looks normal.

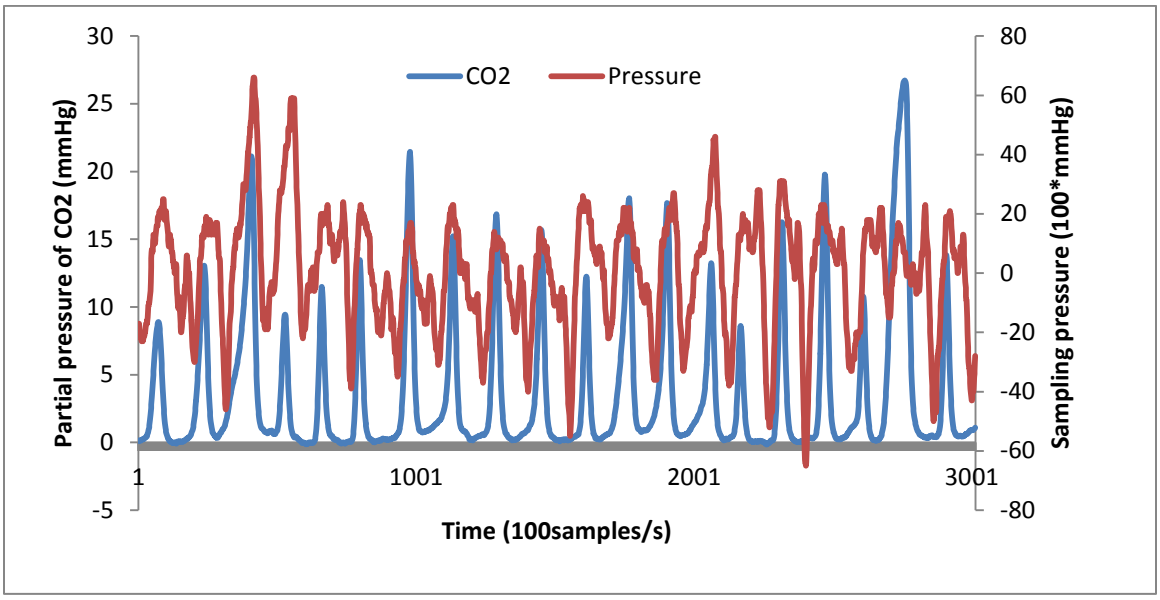

Figure 30: Signals recorded during slow breathing. The CO_2 and pressure signals recorded in the presence of 5 LPM of O_2 when the subject was taking slow breaths are shown. The pressure signal has double peaks during expiration almost in every breath.

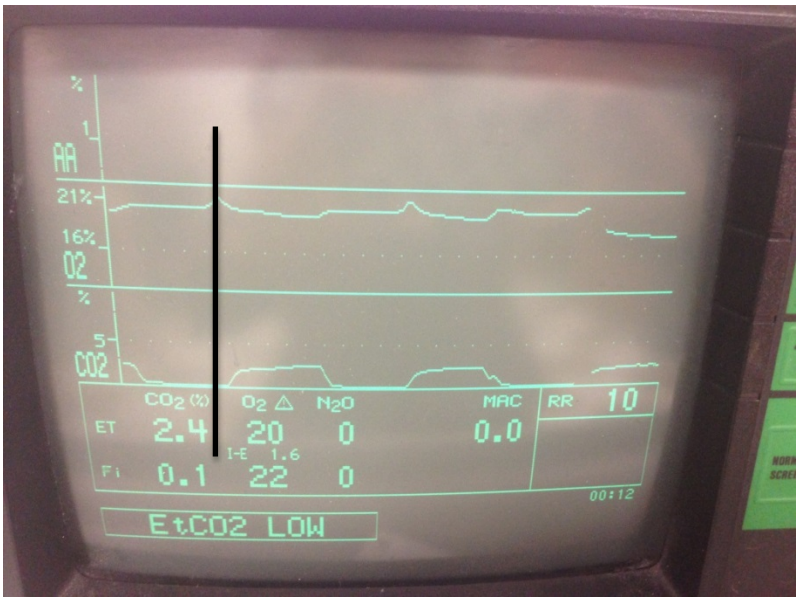

Figure 31: Screen shot from the Capnomac Ultima. The screen shot depicts the changes in the O_2 and CO_2 concentrations during a few breaths, as observed in a human volunteer. It can be seen that right before the capnogram rises up, as the dead space is being cleared, there is a peak in the O_2 concentration (as marked by the black line). The timing of this peak coincides with the peak observed during the beginning of expiration in the sampling pressure signal.

a second peak observed in the pressure signal at the beginning of expiration.

2.4 Confirming Viscosity Theory

Three important gases involved in the process of breathing include O_2, CO_2, and water vapor. Their respective viscosities are 0.21 mPoise, 0.15 mPoise, and 0.68 mPoise. If viscosity has an impact on the morphology of the recorded signals, then all three gases must influence the signals differently. Experiments were conducted with all three gases separately and the signals were recorded to test this hypothesis.

2.4.1 Experiment-1: With O_2

2.4.1.1 Design. Varying concentrations of O_2 were delivered and the sampling pressure and flow signals were recorded. The LoFlo cannula was placed in the outlet port of the ventilator. The ventilator has an O_2-air mixer which helps to switch between air (21% O_2) and higher levels of O_2. The experiment does not involve breaths and hence, the ventilator was not used for this purpose. The experimental set-up is represented in Figure 32. O_2 concentration was initially set to 21% (as in air). It was then increased in steps of 20% (40%, 60%, 80%, and 100%), and switched back to 21% after every step increase. Signals were recorded in each 21% step for 1 minute and each of the higher concentration steps for 1.5 minutes. The pattern of concentration change is depicted in Figure 33.

2.4.1.2 Results. It was observed that the sampling flow increased after an increase in O_2 concentration. A drop in the sampling pressure was seen around the same time. Refer to Figure 34. With higher concentration, the magnitude of the change in the signals

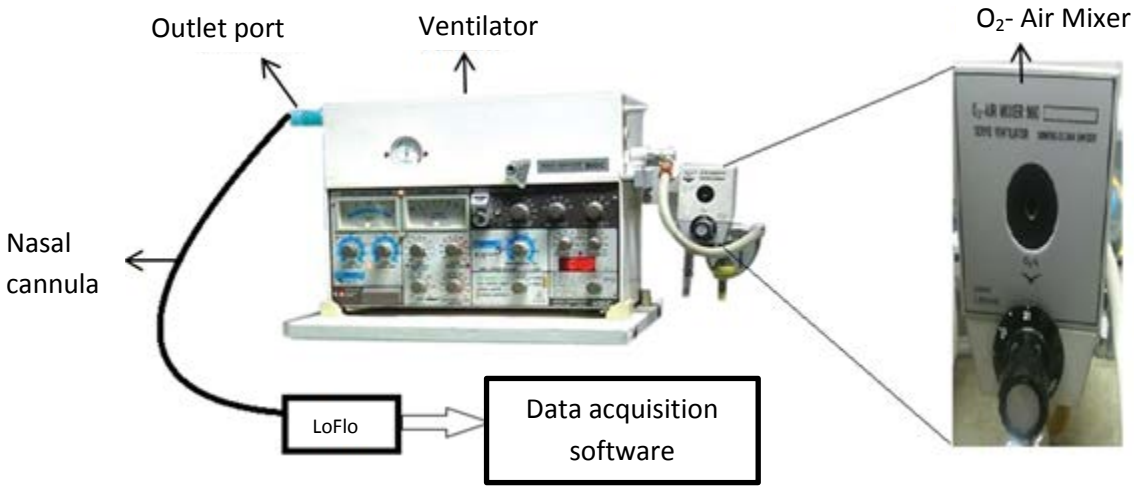

Figure 32: Experimental set-up for testing effects of O_2. The sampling cannula was placed in the outlet port of the ventilator which delivered different concentration of O_2 using the O_2-Air mixer (zoomed in).

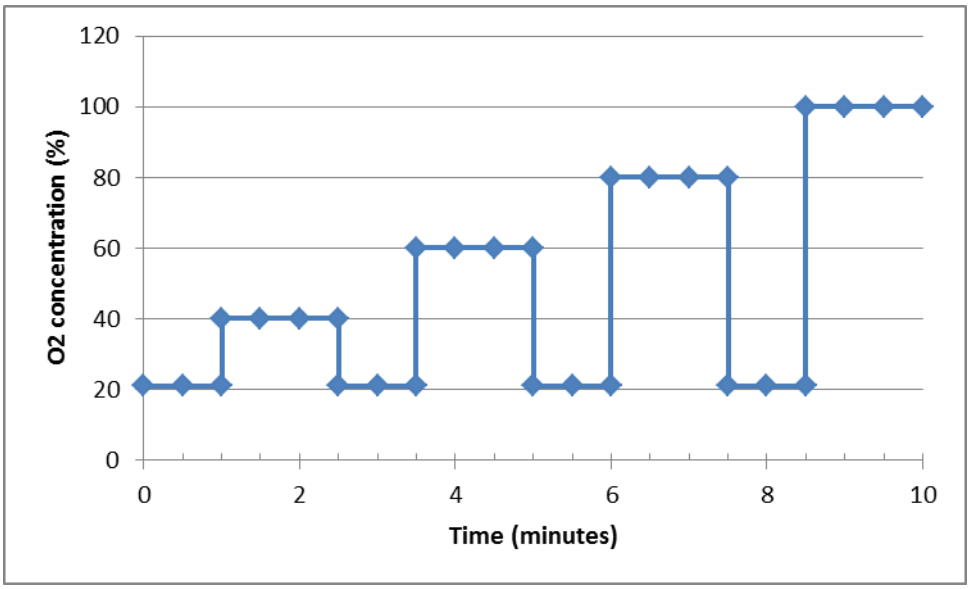

Figure 33: Pattern of change in concentration of O_2. The chart shows the concentration of O_2 supplied by the O_2-air mixer in the ventilator during different times of the experiment.

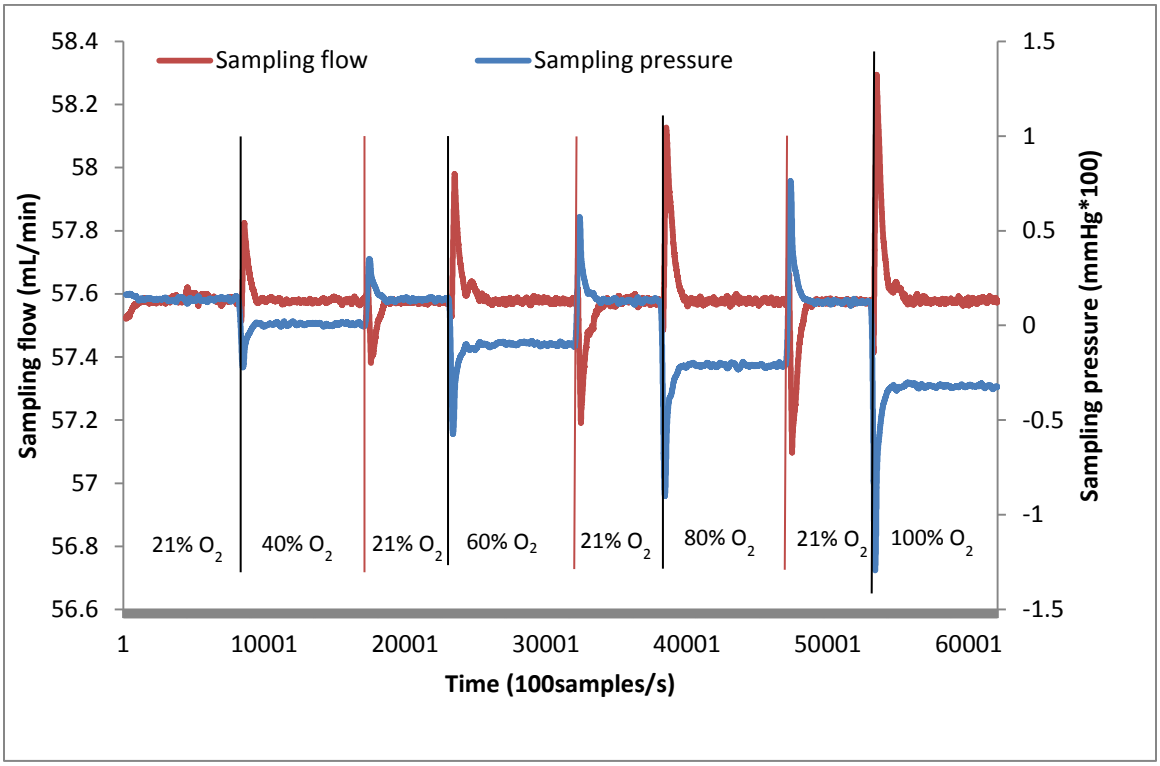

Figure 34: Effect of changing O_2 concentration on sampling pressure and sampling flow signals. The sampling pressure decreased and sampling flow increased on increasing O_2 viscosity. The baseline of the pressure signal dropped to a more negative value on introducing O_2 in concentrations higher than 21%. The flow signal returned to its baseline after the initial increase.

was higher. The amplitude of the positive swing observed in the flow signal increased by 4 times on changing the concentration of O_2 from 40% to 100%. For the same change in concentration, the amplitude of the negative swing observed in the pressure signal increased by 5 times. It should also be noted that while the sampling flow returned to baseline after a momentary increase, on increasing O_2 concentration, there was a negative shift in the baseline of the sampling pressure at O_2 concentrations greater than 21%.

2.4.1.3 Discussion. The sampling pressure is a measure of circuit pressure upstream of the flow meter. With higher concentrations of O_2, the viscosity of the gas increased. This led to a more negative sampling pressure throughout the duration of sampling of the more viscous gas. However, with an increase in viscosity, the pressure drop across the flow sensor increased. This implies a consequent increase in the sampling flow (refer to Equation (2)). The PWM-based feedback action is activated in an effort to contain the growing sampling flow rate. This brings the sampling flow back to the baseline. The pump constantly makes adjustments to its speed to keep the pressure drop and sampling flow a constant. In summary, as long as a gas of viscosity higher than that of air is being sampled, the sampling pressure is lower than usual. Though an initial increase in sampling flow is witnessed, it is restored to its original value by the feedback action of the pump.

2.4.2 Experiment-2: With CO_2

2.4.2.1 Design. A CO_2 waveform generator was programmed to introduce different concentrations of CO_2 into the LoFlo system. The generator varies the partial pressure of CO_2 by injecting a different amount of CO_2, as programmed, into a constant

stream of O_2. Concentration was increased in steps of 10 mmHg up until 70 mmHg and after each increase, it was returned to a baseline value of 0 mmHg. At each level, sampling pressure and sampling flow signals were recorded for 90 seconds. The experimental layout is depicted in Figure 35.

2.4.2.2 Results. The recorded sampling pressure signal and the measured sampling flow signal are displayed in Figures 36 and 37 along with the CO_2 concentration pattern during the experiment. The sampling pressure signal increased on increasing the concentration of the gas and vice versa. As the concentration of the gas increased, the magnitude of the swing in the signal increased. The sampling flow did not show any appreciable change with changing CO_2 concentration.

2.4.2.3 Discussion. The viscosity of CO_2 is 17% less than that of air. Hence, the sampling pressure increases. The less viscous gas also causes a lower pressure drop across the flow sensor than what would be observed with air. This in turn slows the sampling flow accordingly. However, no change was observed in the recorded flow signal. The units of CO_2 concentration in the graph in Figures 36 and 37 is mmHg. The atmospheric pressure in Utah is about 640mmHg. Hence, the percentage of CO_2 even at the maximum recorded concentration of 70 mmHg is about 11%. This might not be big enough to produce apparent swings in the measured flow.

2.4.3 Experiment-3: With Water Vapor/ Humidity

2.4.3.1 Design. A ConchaTherm-III (Hudson RCI Teleflex Inc., North Carolina, USA) was used to induce 100% humidity in the sampling tube at 27°C, 30°C, and 33°C and the sampling pressure and flow signals were recorded from the LoFlo system. The

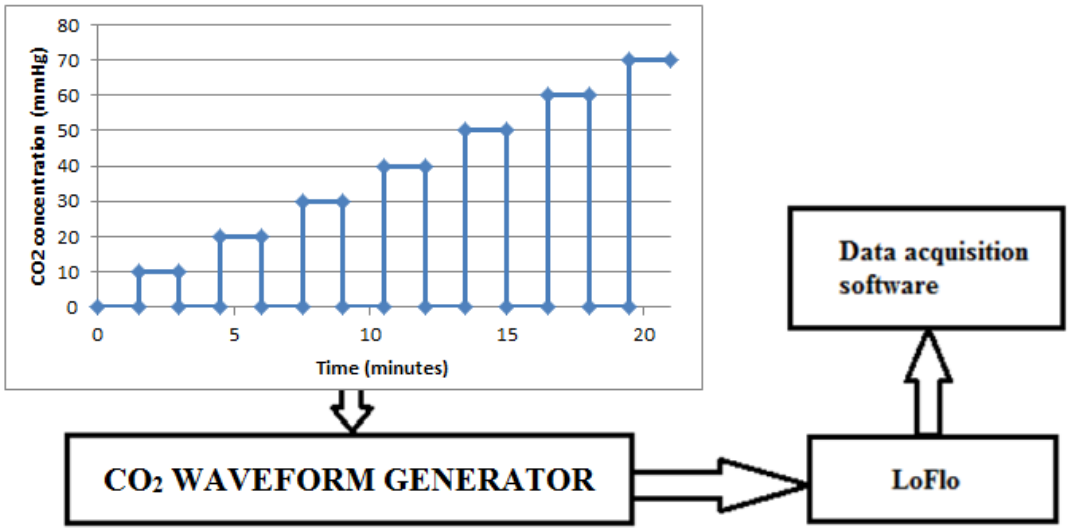

Figure 35: Experimental set-up to test effects of CO_2. The schematic shows the layout of the experiment to test how the sampling flow and pressure signals respond to different concentrations of CO_2. The chart represents the concentration of CO_2 introduced into the capnometer at different instants of the experiment.

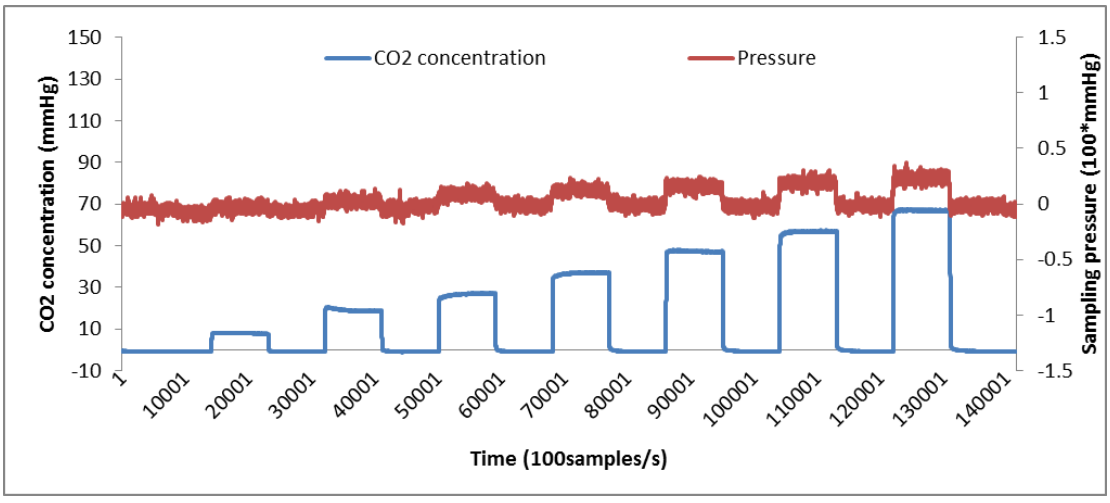

Figure 36: Sampling pressure signal at different CO_2 concentrations. An increase in the pressure signal was observed with increasing the concentration of CO_2.

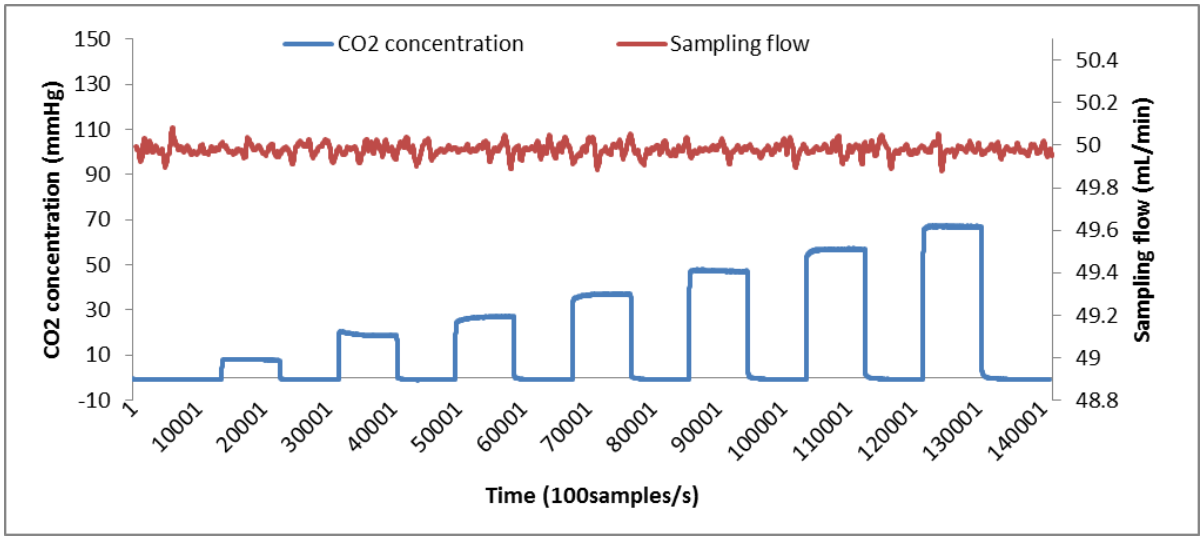

Figure 37: Sampling flow signal at different CO_2 concentrations. The flow did not change significantly with increasing the concentration of CO_2. Random fluctuations were seen throughout the experiment.

sampling tube was placed in the outlet of the humidifier and then in the outlet port of the ventilator as a way of alternating between dry air and humidified air. Signals were recorded in the presence of humid air for 2 minutes and dry air for 2 minutes after baseline restoration. Table 2 explains the experimental design. This was done twice during each temperature setting. The layout of the study can be seen in Figure 38.

2.4.3.2 Results. The results are displayed in Figures 39, 40, and 41. The sampling flow signal did not show significant swings in the presence of humid air. The baseline of the pressure signal became more negative on switching from dry air to humid air. At 30 °C and 33 °C, the change in the amplitude of the signal in the presence of humidity was 2.5 times and 3 times that recorded at 27 °C. At 33 °C, it took some time for the sampling pressure signal to return to baseline on switching to dry air from humid air.

2.4.3.3 Discussion. The viscosity of water vapor is higher than air; hence, the results were expected to be similar to those obtained with O_2. While O_2 is 1.2 times as viscous as air, vapor is 3.8 times more viscous than air. Thus, the results were supposed to be magnified compared to those from experiment-1. The water vapor content of humid air depends on temperature and this is described by the graph in Figure 42. [3] The derived mathematical relationship was used to determine the percentage of water vapor in the humidified air during the experiment. The corresponding levels of water vapor at temperatures of 27°C, 30°C, and 33°C is 2.21%, 2.76%, and 3.45%, respectively. The percentage of vapor in the sampling gas is very less even at 33°C, compared to the concentration of O_2 in experiment-1. This is probably the reason why no change was observed in the sampling flow signal and the change in amplitude of the sampling

[3] http://web.gccaz.edu/~lnewman/gph111/topic_units/Labs_all/Water%20Vapor%20Capacity%20of%20Air.pdf

Table 2: Experimental layout to test the effects of water vapor on the sampling pressure and sampling flow signals.

Time (minutes)	Position of cannula
2	Ventilator
2	Humidifier
2 minutes after baseline restoration	Ventilator
2	Humidifier

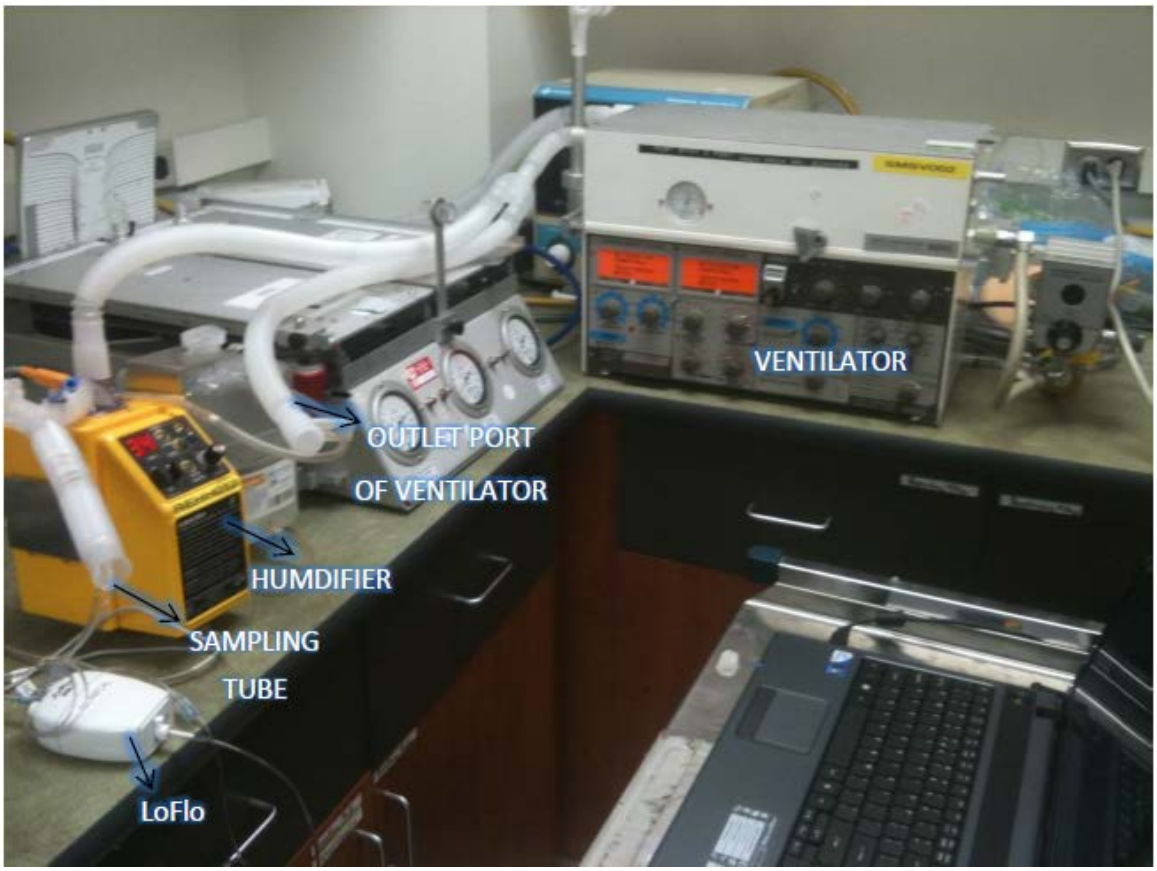

Figure 38: Experimental set-up to test effects of humidity. The schematic shows the layout of the experiment to test how the sampling flow and pressure signals respond to different levels of humidity. The sampling tube was placed alternatingly in the outlet of the humidifier and ventilator to switch between humid and dry air, respectively.

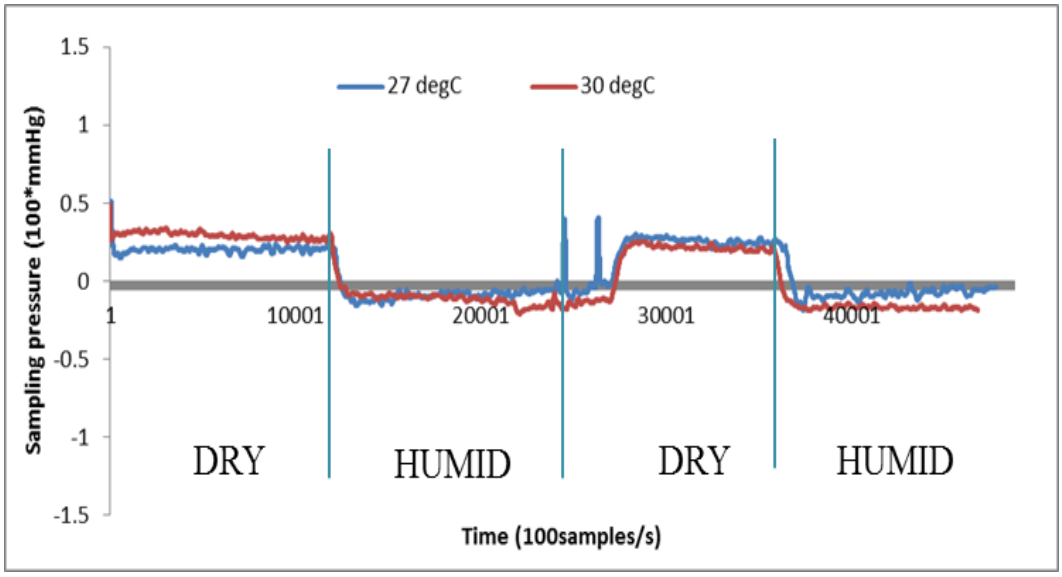

Figure 39: Sampling pressure signals at 27°C and 30°C. The sampling pressure signals dropped when the sampling gas was switched from dry air to humid air. With increase in temperature, the drop in pressure was 2.5 times higher.

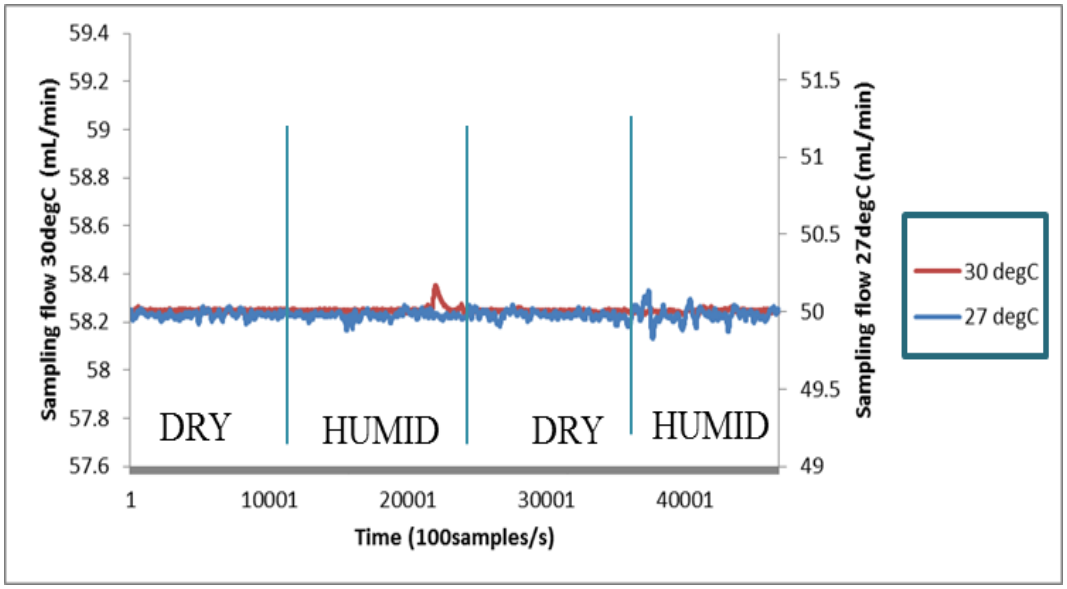

Figure 40: Sampling flow signals at 27°C and 30°C. The flow signals did not show a significant change on changing the humidity content of the sampling gas.

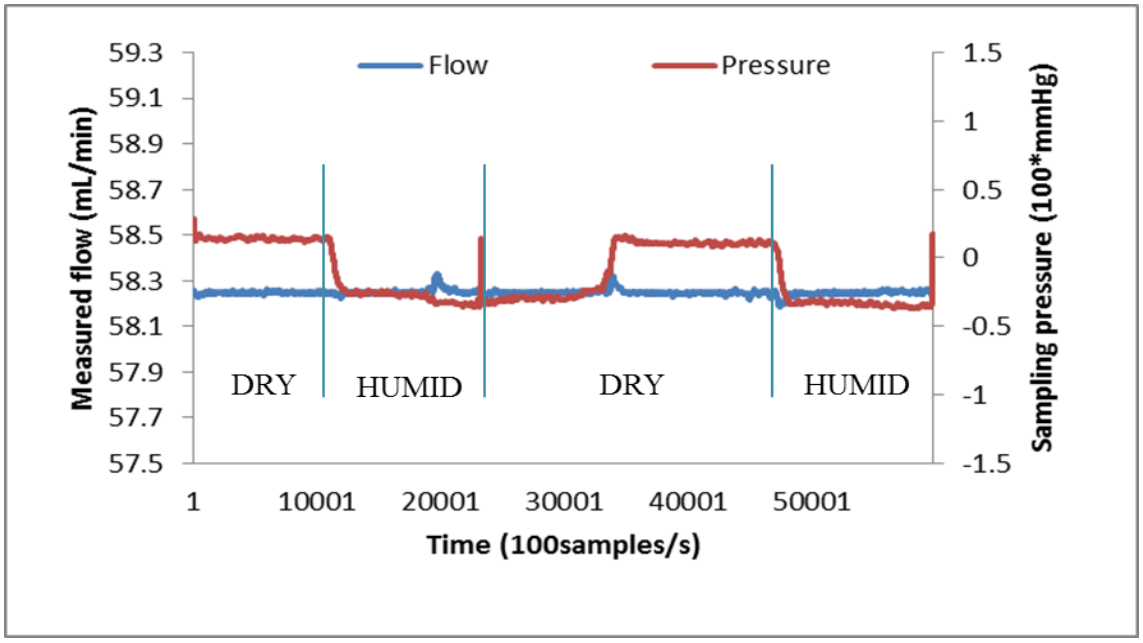

Figure 41: Sampling pressure and flow signal at 33 °C. The change in sampling pressure at increased humidity was 3 times the change observed at 27 °C. The flow signal remained largely unchanged during the experiment.

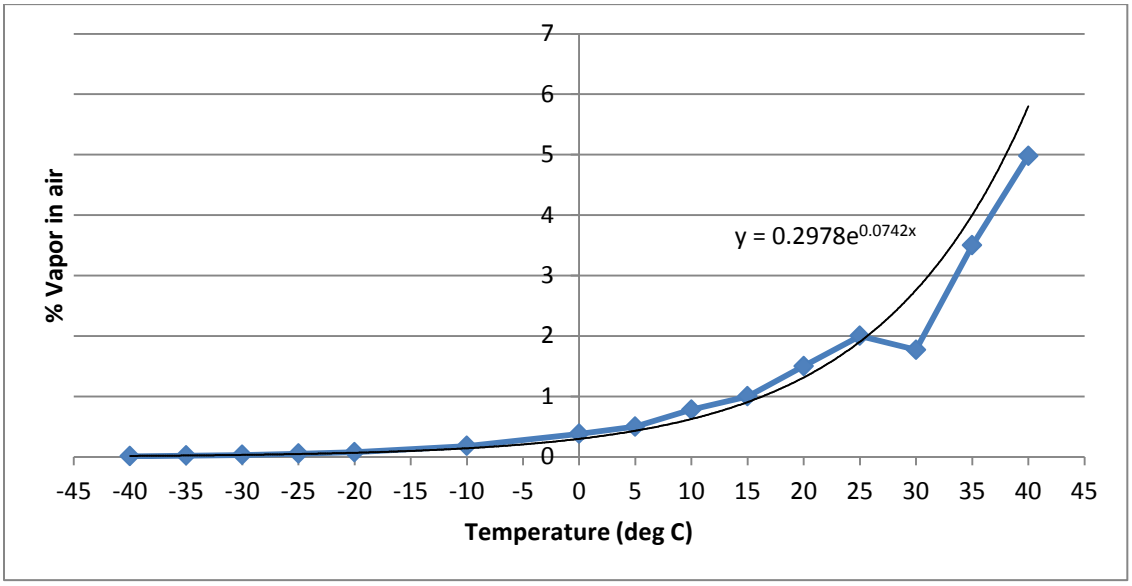

Figure 42: Relationship between temperature and water vapor content. The graph explains how the percent vapor changes with temperature. The displayed equation describes the mathematical relationship between the variables.

pressure swing was not greater than what was observed in the presence of O_2. The reason for the delayed baseline restoration at 33°C might probably be that it took longer than usual to completely wash away the humid air from the sampling system.

2.4.4 Conclusion

The change in the amplitude of the pressure signal obtained on switching from different percentages of O_2 or CO_2 or water vapor to air is displayed in Figure 43. The slope of the curves might be suggestive of the viscosity of the corresponding gases. Water vapor, having the highest viscosity, has the greatest slope, followed by O_2. CO_2, being less viscous than air, has a negative slope. The slope in the equation depicted in the graph does not match with the theoretical value because other factors are involved in the relationship between the variables.

The findings discussed in the previous sections confirm the viscosity theory and that all three gases have an effect on the magnitude of the pressure signal. To summarize, the presence of O_2 during inspiration causes the sampling pressure to drop to a more negative value than it would with air (as indicated by a negative baseline shift in experiment-1), causing an increase in the peak-to-peak amplitude of the signal. As the subject starts to expire, a new phase of breathing begins and respiratory pressure increases. As the dead space is cleared, O_2 comes out and the flow meter senses a more viscous gas, causing a drop in the sampling pressure. This was observed as the first peak during expiration. Once the dead space clears, humidified CO_2 comes out. While water vapor is expected to cause a drop in sampling pressure, the presence of CO_2 is supposed to increase the sampling pressure. However, no additional spikes or swings were

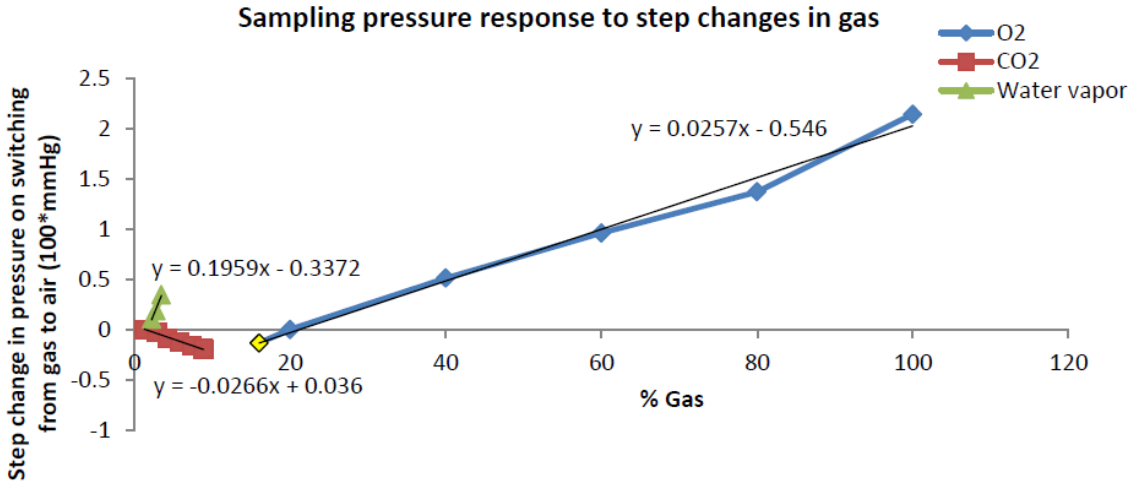

Figure 43: Summary of the viscosity theory. The graph shows the changes produced in the sampling pressure signal on switching from CO_2, O_2, or water vapor to room air. The slope of the curves is reflective of the viscosity of the gas relative to air.

observed in the signal and it appeared normal during the rest of the breathing cycle. The probable explanation might be that the effect of these two gases cancels out each other. At body temperature, the water vapor content is 4.64% (see Figure 42). The experiments were conducted in Salt Lake City, Utah, which is at an elevation above sea level and the expired CO_2 is normally close to 6%. The lines in Figure 43 are shown the way they are to represent the relative viscosity of the gases. They represent the effect on the sampling pressure signal on changing from the test gas to air. During breathing, the opposite change has to be considered ─ change from air to test gas. Taking this into consideration, water vapor at body temperature would produce a decrease of 0.57 units in the sampling pressure signal while 6% CO_2 corresponding to a rise of 0.12 units in the signal. This should ideally produce a spike of 0.45 units in the negative direction. However, no such spike was observed. A possibility is that the gas cools down to room temperature by the time it reaches the sensor in the monitor. In this case, the water vapor causes a decrease of 0.07 units, resulting in an overall increase of 0.05 units which is too small to be observed.

2.4.5 Significance of the Finding

The presence of O_2 distorts the sampling pressure signal and causes double peaks which will result in double counting during calculation of breath rate, leading to false alarms. If O_2 can be detected from the sampling pressure and the sampling flow signal successfully, then it can be put to use to alert clinicians when supplemental O_2 is not being delivered to nonintubated patients in the ICU or sedated patients in the OR. An important consequence of the viscosity theory is that the amplitude of the signals no

longer holds any clinical significance. It gets falsely elevated due to the presence of O_2. This is yet another piece of information that can be conveyed to the clinician. The next part of the project focusses on detecting O_2 from the signals and testing to see if the sampling pressure signal can be used to detect apnea accurately even when supplemental O_2 is being sampled.

CHAPTER 3

TESTING WITH CLINICAL DATA

3.1 Clinical Data Collection

Data were collected from 31 sedated patients undergoing colonoscopy with supplemental O_2 delivered at 6 LPM. If the patient had a history of respiratory illness, additional O_2 was supplied through a nasal mask. Besides the capnogram, sampling pressure, and sampling flow signals collected from the capnometer, respiratory pressure signals were collected using thoraco-abdominal bands. The nasal airway pressure was also recorded using a Non-invasive Cardiac Output (NICO) monitor (Novametrix Medical Systems Inc., Wallingford, U.S.A). The patient's blood O_2 saturation (SpO_2) was documented using a pulse oximeter. This was an IRB-approved study and the data were used in the following parts of the project.

3.2 Detection of O_2 from Sampling Pressure and Sampling Flow Signals

3.2.1 Method

The sampling pressure and sampling flow signals were used to develop an algorithm to detect supplemental oxygen (O_2) in a breath. In order to compile a training

data set, respiratory data were collected from nine volunteers using the sidestream capnometer with air or O_2 delivered at 2 LPM through a nasal cannula. These data were analyzed to establish the criteria or threshold for the detection of O_2. The 31 patient data files were used to test the algorithm and comprised the testing data set. The notes taken during data collection indicated that O_2 was supplied throughout the colonoscopy procedure in all 31 cases. Hence, an accurate algorithm would detect O_2 in all the files.

3.2.2 Algorithm

The algorithm is based on the findings from the viscosity theory. That is, the presence of O_2 increases the amplitude of the sampling pressure and the sampling flow signal, and produces double peaks during expiration. These two features can be detected to confirm the delivery of supplemental O_2 from the respiratory data. As stated earlier, double peaks were not present in every breath and may be completely removed on filtering the signal. Hence, this condition was used as a secondary source of O_2 confirmation, when using the first feature alone does not detect supplemental O_2 in the 31 files.

The average breath time was calculated from the capnogram of each file. This value was defined as the minimum peak-to-peak distance while estimating the time indices of the positive and negative peaks in each breath of the filtered sampling pressure signal. The purpose of defining a minimum peak-to-peak distance was to avoid detecting double peaks which may occur during expiration in the presence of O_2. The value of the sampling pressure signal at these time indices was used to estimate the magnitude of the signal in each breath. The average magnitude, P, was then determined. Since the

sampling pressure and flow signals were aligned in time, the same time indices were used to find the magnitude of the flow signal in every breath, followed by its average, f. The ratio of magnitudes, P/f, was also calculated. The algorithm is depicted in the form of a flow chart in Figure 44.

P, f, and P/f in each file of the training data set was considered to establish the threshold for detection of supplemental O_2. Once the threshold was determined, the same algorithm was applied to the testing data set, and the thresholds were applied to the results to ascertain the presence of O_2.

3.2.3 Results

3.2.3.1 Threshold determination from training data set. The results of the algorithm from the training data set are shown in Figure 45. The X-axis indicates the file number and the supplemental gas delivered during data collection. P, f and P/f value from the files containing air was 1.3 ± 0.4 mmHg, 0.0035 ± 0.001 V, and 540 ± 140 mmHg/V, respectively. The corresponding values for the last three files with O_2 were 1.6 ± 0.2 mmHg, 0.006 ± 0.003 V, and 355 ± 35 mmHg/V, respectively. From the previous chapter, it is known that P and f are greater with O_2 than with air. This in turn implies that P/f should be lesser with O_2 than with air. Combining these facts with the average parameter values stated above, the thresholds were defined as follows-

It can be said that O_2 is present in a breath if-

1. $P > 1.5$ mmHg or,
2. $f > 0.005$ V or,
3. $P/f < 400$

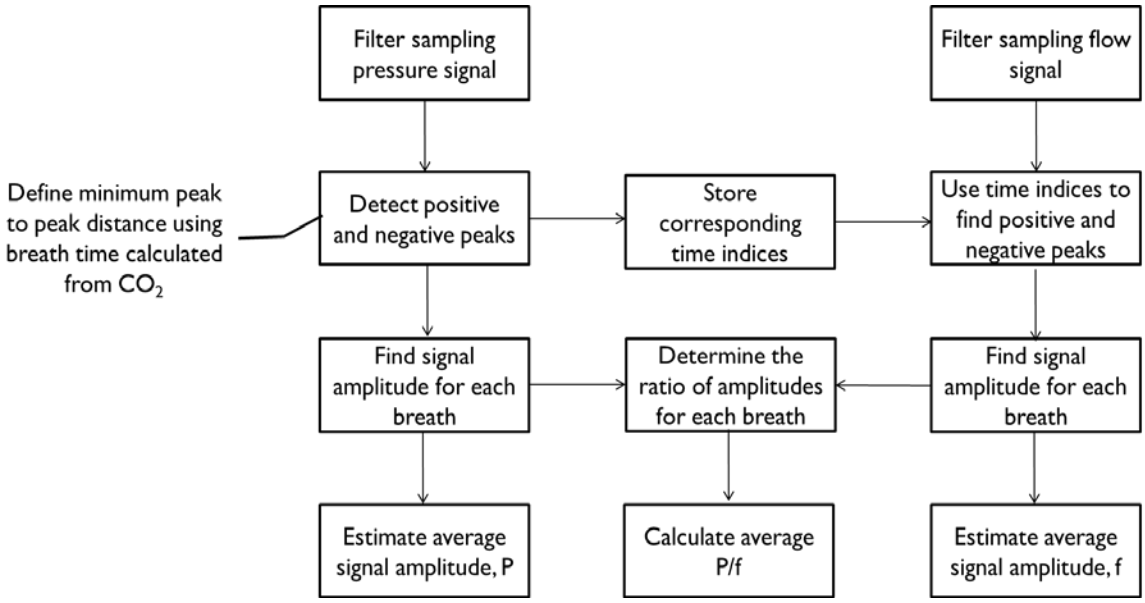

Figure 44: O_2 detection algorithm. The detection algorithm is based on the effects of O_2 on the sampling pressure and flow signals. The three parameters obtained by the algorithm- P, f, and P/f- are used to establish thresholds to ascertain the presence of O_2 in every breath of the testing data file.

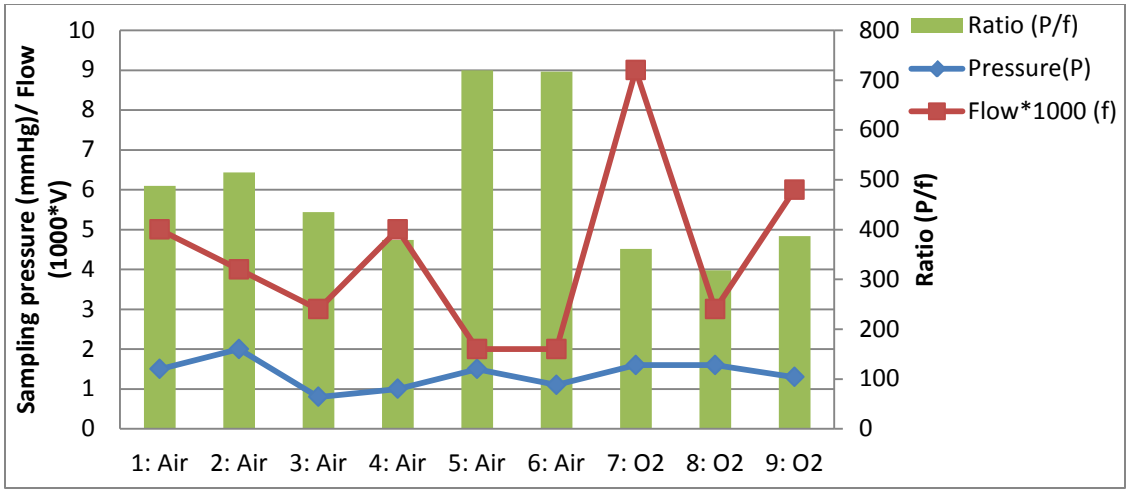

Figure 45: Results from the training data set. The chart shows the average P, f, and P/f values obtained for each of the 9 files in the training data set. The X-axis indicates the file number and the supplemental gas delivered during data collection. An average value of these parameters in the presence of O_2 and air were calculated to determine the threshold for classification of files as having O_2 or not.

One way of classifying the files is by using each threshold individually to confirm the presence of O_2. For example, if P alone is used, then O_2 is present only if the average P of the test file is greater than 1.5 mmHg. The f and P/f values of the file are not taken into consideration. Similar definitions are made using f and P/f as the sole deciding criterion. A second method of classification is by ascertaining the presence of O_2 even if one of the threshold conditions is satisfied. That is, O_2 is present in the file if P > 1.5 mmHg or f > 0.005V or P/f < 350 mmHg/V. Both methods were tested and the more successful one would be used in future.

3.2.3.2 Results from testing data set. The breath-wise parameter values for one of the patient files are shown in Figure 46. The P, f and P/f values obtained for each of the 31 files, along with the corresponding thresholds are shown in Figures 47, 48, and 49. P is higher than the threshold in 54% of the cases, f is greater than the threshold in 77% of the files, and P/f is lower than the corresponding threshold in 87% of the data files. If the algorithm works successfully, it can be used to sound an alarm every time the patient does not receive O_2. Hence, the condition for an alarm is the absence of O_2 as detected by the algorithm. Accordingly, the true positive (TP), true negative (TN), false positive (FP), and false negative (FN) conditions are defined as explained in Table 3. Positive conditions are those that meet the alarm criterion and negative ones are those that do not meet the alarm criterion. Conditions are said to be true if they coincide with actuality and false otherwise. The notes taken during data collection were used along with the obtained results to determine the value for these conditions. These are in turn used to define accuracy and specificity of the classification technique as described in Table 4. Accuracy is a measure of classifier performance while specificity is the proportion of normal data

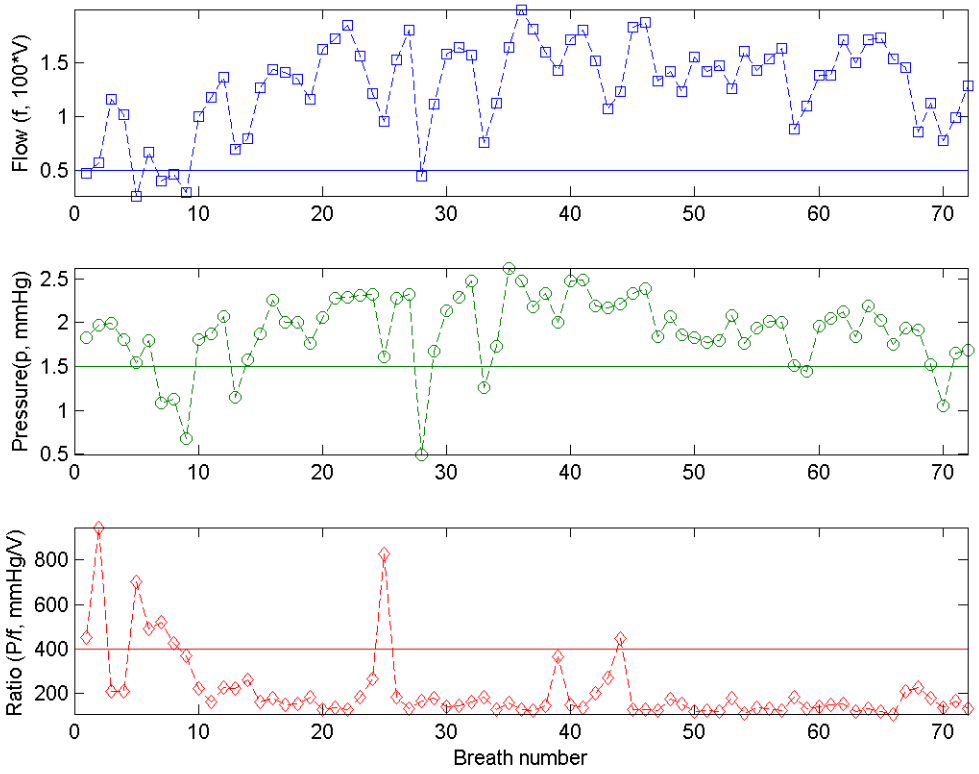

Figure 46: Parameters obtained for one patient file. The f, P, and P/f values obtained by the algorithm for each breath in the patient file are displayed. The solid lines in each plot represent the threshold for the respective parameters. In this case, f and P were higher than their thresholds in 93% and 90% of the breaths while P/f was lower than its threshold in 89% of the breaths.

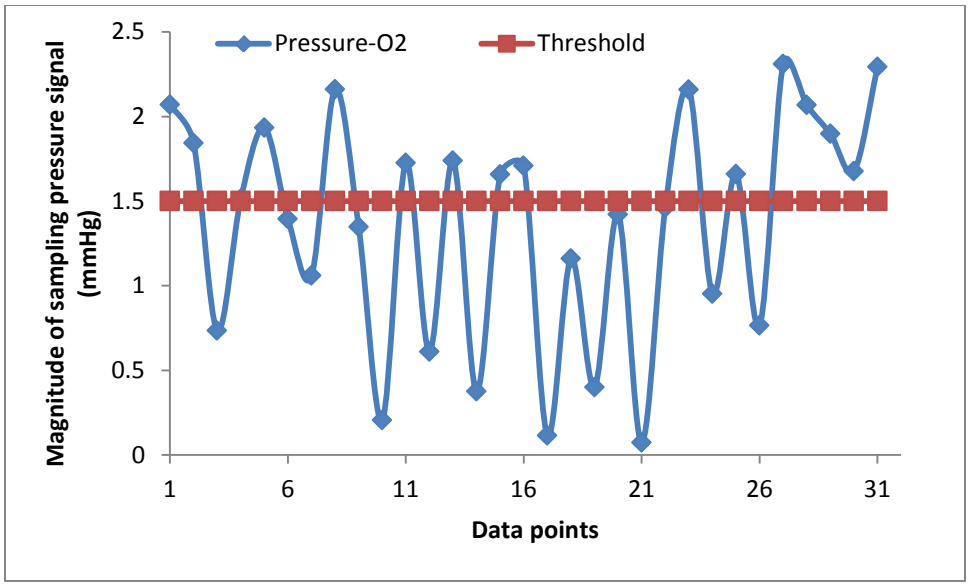

Figure 47: Trend of P in the testing data set. The P obtained for each of the files in the testing data set is shown, with the threshold marked in brown. Unlike expectations, it was found that P was higher than the predetermined threshold in only 52% of the files.

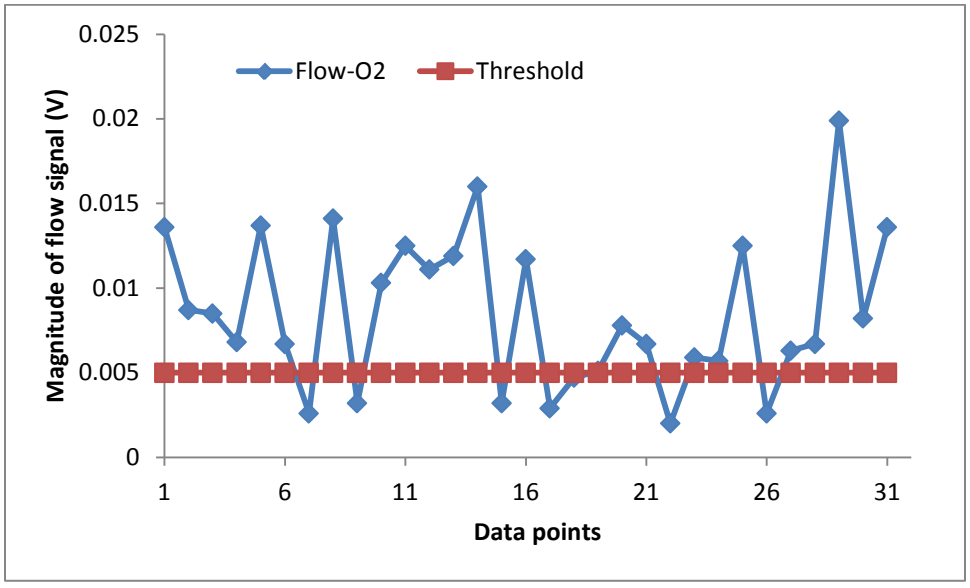

Figure 48: Trend of f in the testing data set. The blue points indicate the f obtained by the algorithm for each of the files in the testing data set and the brown line indicates the threshold. This criterion confirmed the presence of O_2 in 81% of the files.

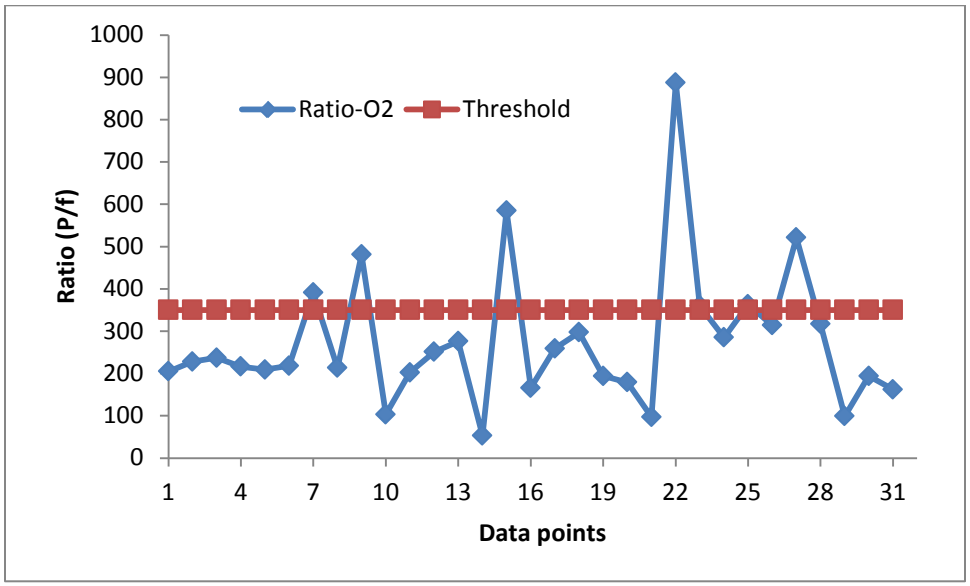

Figure 49: Trend of P/f in the testing data set. This parameter is a combination of the previous two and is hence expected to perform better than P alone or f alone. As expected, it detected O_2 in 87% of the cases, the highest of the three parameters. The blue and brown lines indicate the value obtained by the algorithm and the threshold, respectively.

Table 3: Definition of TP, FP, TN, FN conditions for detection of O_2 from breaths.

Condition	**Definition**
True positive (TP)	No O_2; algorithm confirms absence of O_2
False positive (FP)	O_2 present, algorithm fails to detect O_2
True negative (TN)	O_2 present; algorithm confirms presence of O_2
False negative (FN)	No O_2; algorithm wrongly detects O_2

Table 4: Definition of performance parameters of the algorithm.

Parameter	**Definition**
Accuracy	(TP + TN) / (TP + FP + TN + FN)
Specificity	TN / (TN + FP)

(defined as the files with O_2) classified as normal. The value of the TP, FP, TN, and FN are determined for both methods of classification and displayed in Table 5. TP and FN are zero since O_2 was delivered throughout data collection in all 31 cases. The corresponding accuracy and specificity values are shown in Table 6. It was determined that method-2 had the highest accuracy and specificity of 94% and yielded the best results. This technique, however, could not detect O_2 in two files. When the unfiltered sampling pressure signals from these files were analyzed, both showed incidence of an additional spike during expiration, confirming that O_2 was indeed present. The signal from one of the two files is shown in Figure 50. The arrows indicate the spike due to the presence of O_2.

Hence, it can be concluded that O_2 can be successfully detected from the sampling pressure and flow signals and this would be a reliable way of alerting clinicians about the absence of supplemental O_2.

3.3 Breath Detection Using Sampling Pressure and CO_2 Signals

The last part of the project involved determining how effective the pressure signal was in detecting apnea relative to the capnogram. Breath rate was calculated from the pressure signal and capnogram and the results were compared. Absence of a breath was interpreted as apnea. Clinical respiratory data from the IRB-approved study was used in analysis.

Table 5: Values of TP, FP, TN, and FN obtained for the algorithm by method-1 (individual parameters) and method-2 (all three parameters together)

Condition	**P alone**	**f alone**	**P/f alone**	**P or f or P/f**
TP	0	0	0	0
FP	15	6	4	2
TN	16	25	27	29
FN	0	0	0	0

Table 6: Measures of performance of method-1 and method-2 of classification

Parameter	P alone	f alone	P/f alone	P or f or P/f
Accuracy	52%	81%	87%	94%
Specificity	52%	81%	87%	94%

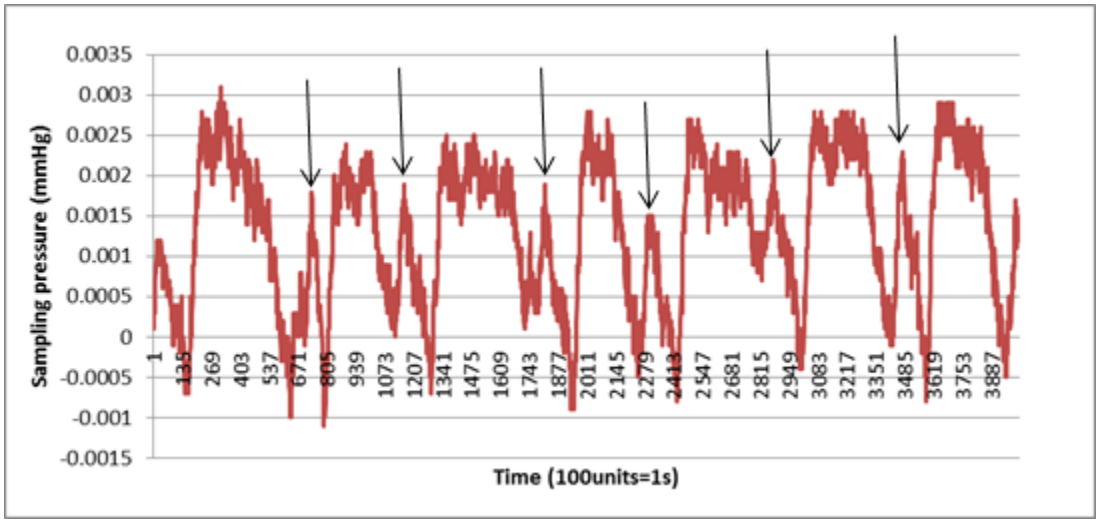

Figure 50: Presence of double peaks in the sampling pressure signal. This signal was taken from one of the two files where O_2 could not be detected by the algorithm. The presence of an additional peak during expiration was observed in most parts of the file. The double peak during expiration is a feature of the pressure signal in the presence of O_2, confirmed by the viscosity theory.

3.3.1 Algorithm

A moving average filter was applied to the sampling pressure signal to remove any spikes observed during expiration before it can be used in the algorithm to detect breaths. The least squares alignment algorithm was used to align the aforementioned signals so that a useful comparison can be made between the results obtained from the two signals. The amplitude of the signals during each breath was determined and the average amplitude was calculated for each data file. The number of breaths in each 30-second interval of the file was estimated. A period of apnea was declared if one of the following conditions were met-

1. The amplitude of the detected deflections during a 30-second interval was less than the average amplitude minus one standard deviation, OR
2. The standard deviation of the signal during the interval was less than 25% of the standard deviation of the entire signal

The first condition eliminates small breaths as defined by the mean and standard deviation, while the second condition helps the algorithm ignore small fluctuations that may occur during apnea. Only when both the above conditions were false was the deflection considered as a breath. Figure 51 depicts the algorithm as a flow chart. It should be noted that an apneic episode was detected only if no breaths were observed for an entire 30-second duration. Apnea, as detected by either signal, was confirmed by visualizing the thoraco-abdominal band signals recorded during the interval.

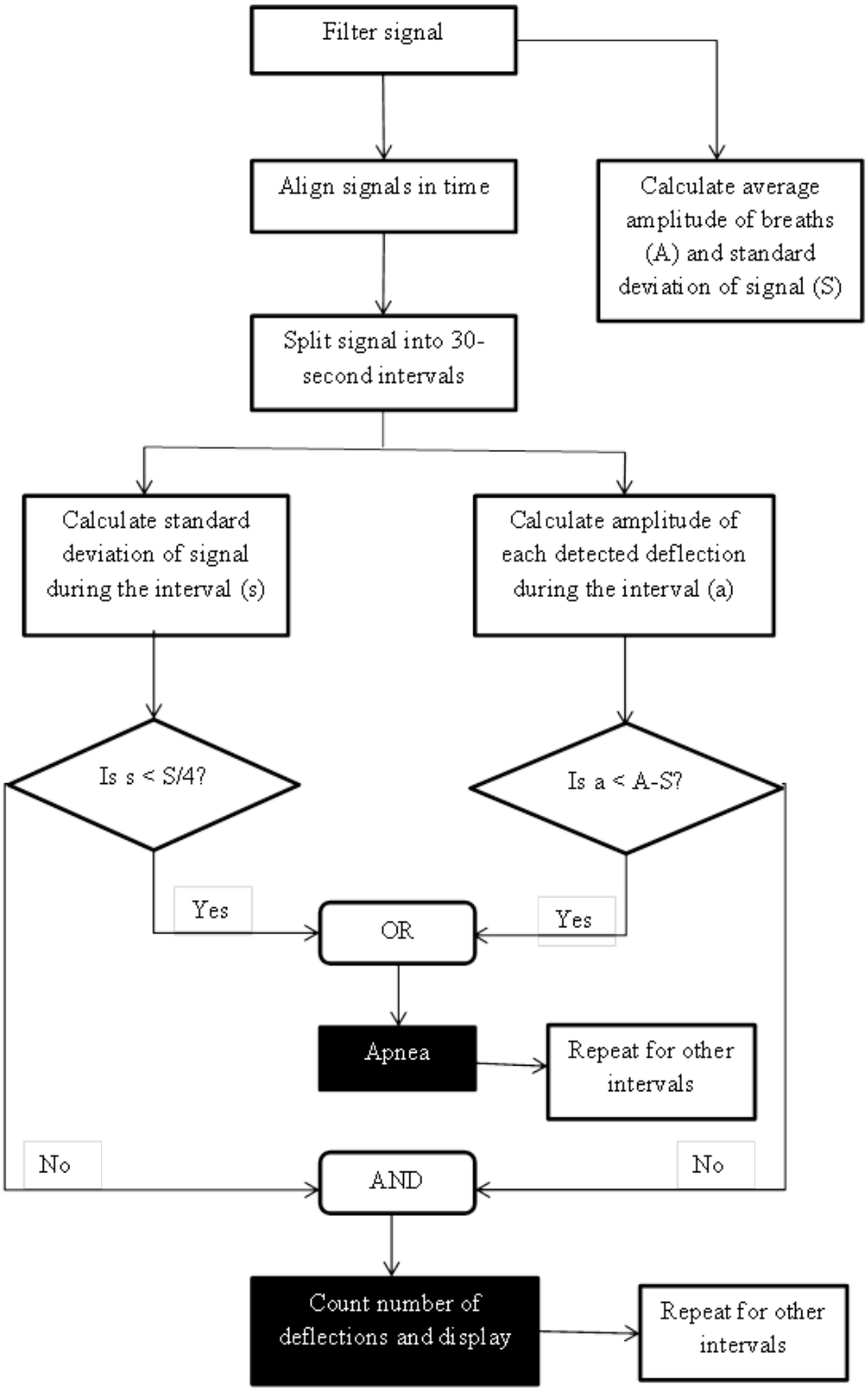

Figure 51: Breath detection algorithm. The flow chart depicts the various steps followed in detecting breaths and apnea from the capnogram and the sampling pressure signal. This algorithm finds the number of breaths in 30-second intervals only if both the conditions for apnea are false (as represented by the AND block).

3.3.2 Results

The average R^2 value between the results calculated from the sampling pressure signal and the capnogram for the 31 files was 0.67 ± 0.21. The number of breaths observed during each 30-second interval in one of the patient files is shown in Figure 52. In the figure, apnea was detected by both signals at 4 points. After verification with the thoraco-abdominal band signals, it was confirmed that the patient had apnea during all 4 intervals. If there is an alarm every time apnea is detected by the algorithm, positive events are defined as those intervals during which apnea was detected. Negative events occur when the algorithm detects breath(s) during an interval. The conditions are said to be true if they coincide with the fact; otherwise they are false. With the thoraco-abdominal band signals as the reference, the TP, FP, TN, and FN values were estimated for both signals. The definition of these conditions and their corresponding value as obtained from the individual signals are displayed in Table 7. Performance parameters of the algorithm are defined and estimated in Table 8. In addition to those described in Table 3, sensitivity is also calculated here. Sensitivity is the proportion of abnormal data (intervals in which apnea was detected) classified as abnormal. The pressure and CO_2 signals detected apnea 99% and 98% of the time with a specificity of 100% and 99%, respectively. While the sensitivity of the capnogram was 96%, the sampling pressure signal had a sensitivity of 69%.

3.3.3 Discussion

It is important to note that the sampling pressure signal gives 60% less false positive results when compared to the capnogram. In two of the eight intervals of apnea

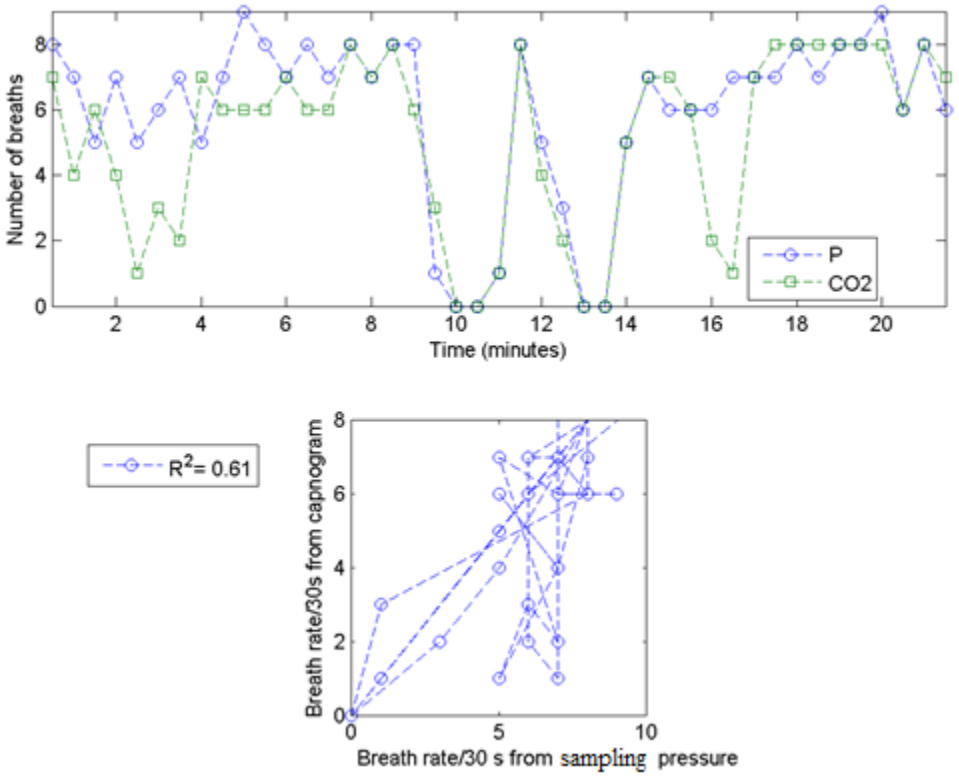

Figure 52: Results of breath detection algorithm. The chart displayed on top shows the breath rate obtained for each 30-second interval from the CO_2 (green) and pressure (blue) signals. Minutes 10, 10.5, 13, and 13.5 indicate apnea detected by both signals. The second plot shows the correlation between the breath rates obtained from both the signals. As indicated, an R^2 of 0.61 was obtained.

Table 7: Definition and values for TP, FP, TN, and FN conditions for detected of apnea by the breath detection algorithm.

Condition	Definition	Value for sampling pressure signal	Value for capnogram
True positive (TP)	No breath; algorithm detects apnea	18	25
False positive (FP)	Breath present; algorithm wrongly detects apnea	2	5
True negative (TN)	Breath present; algorithm detects breaths	1308	1297
False negative (FN)	No breath; algorithm detects breaths	8	1

Table 8: Performance of the signals in detecting apnea.

Parameter	Definition	Pressure signal	Capnogram
Accuracy	(TP + TN) / (TP + FP + TN + FN)	99%	98%
Sensitivity	TP / (TP + FN)	69%	96%
Specificity	TN / (TN + FP)	100%	99%

detected by the capnogram and missed by the sampling pressure signal, the pressure signal showed random deflections that did not obey either of the two predefined conditions for apnea. This caused the algorithm to detect breaths. However, in the remaining six cases, the pressure signal detected one breath. When the signal was visualized in these intervals, it was observed that one peak was present either at the beginning of the period of study or towards the end. This indicates a mismatch in the alignment of the signals. As stated earlier, the alignment algorithm achieves aligning individual breaths and not the inspiratory and expiratory periods of each breath. When the end of expiration is not aligned well enough, the capnogram may have already reached baseline during the last breath before apnea, while the pressure signal is yet to become zero. See Figure 53. This would also occur if CO_2 is washed out by O_2, just before the start of apnea. When the patient starts inspiring after a period of apnea, even if the signals are perfectly aligned, the pressure signals starts to rise while the capnogram does not show any rise in value until the dead space is cleared. One such incident is shown in Figure 54. If results from the sampling pressure signal were considered independently without aligning and comparing with the capnogram, it identified every incidence of apnea with an accuracy of 99% and a sensitivity of 96%.

The pressure signal showed noticeable swings even with minimal respiratory effort, which did not show up on the thoraco-abdominal bands or the capnogram. Hence, additional criteria had to be included for identification of true breaths from the signal. This increased sensitivity of the sampling pressure signal should be kept in mind while designing an algorithm for breath detection.

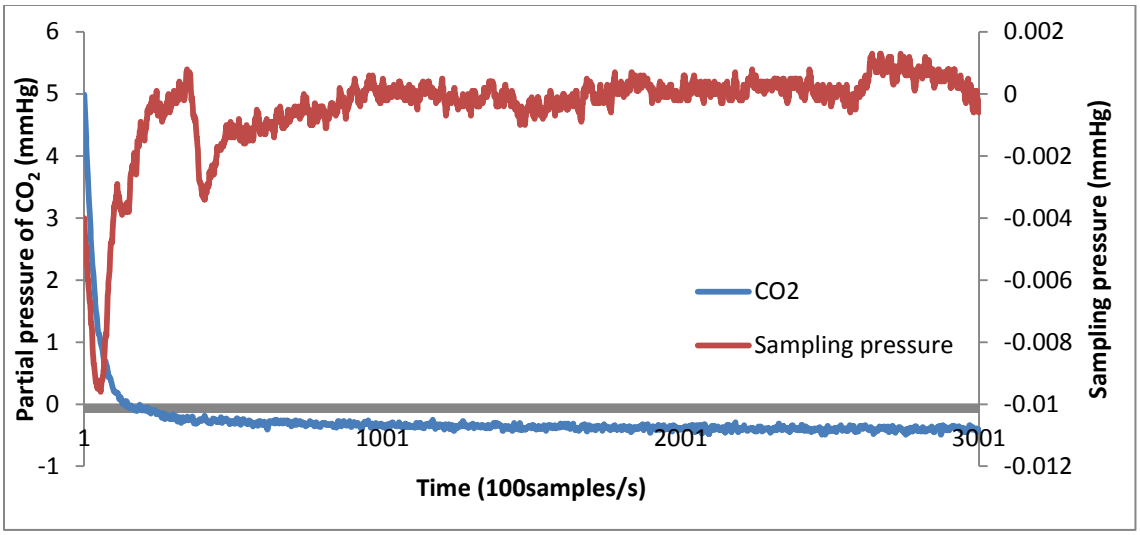

Figure 53: Pressure and CO_2 signals during a period of apnea. The signals shown above were recorded during an interval identified as apnea by the capnogram and not by the pressure signal. It can be seen that the pressure signal failed to detect apnea because of the large swing seen at the beginning of the interval.

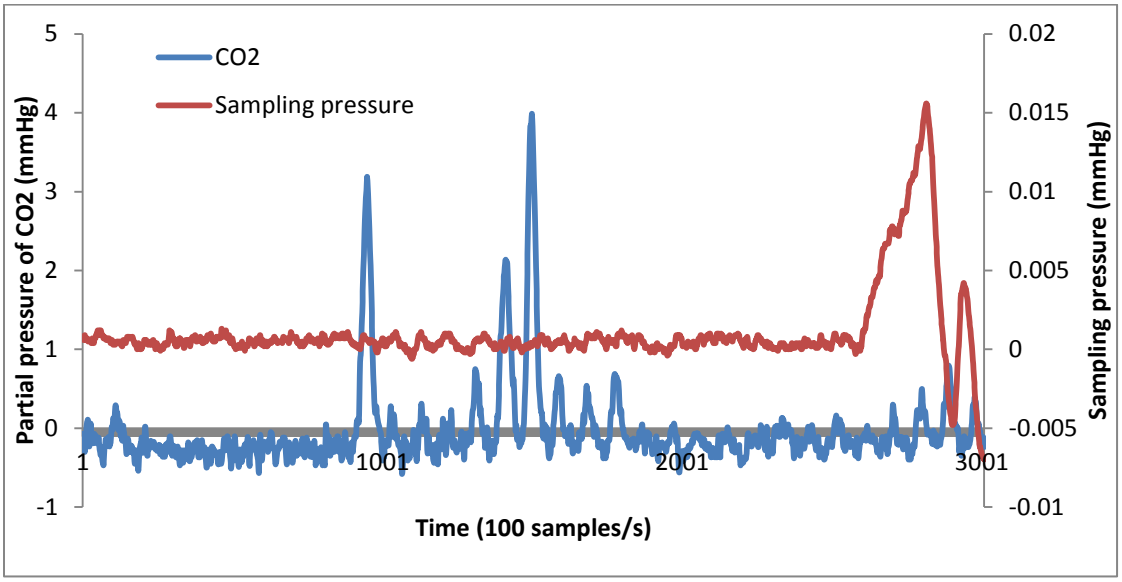

Figure 54: Pressure and CO_2 signals during a period of apnea. The pressure signal detected one breath during this interval due to the deflection towards the end of the interval. The capnogram detected apnea during this period.

CHAPTER 4

CONCLUSION

The purpose of the project was to use the sampling pressure signal in addition to the capnogram to increase the reliability of patient respiratory monitoring. In particular, the goal was to contrast the performance of the sampling pressure signal and the capnogram in detecting apnea accurately in the presence of supplemental O_2. It was found that the pressure signal yielded 60% fewer false positive results than the CO_2 signal, helping reduce the condition leading to alarm fatigue. The pressure signal, being instantaneous, helped detect apnea and respiratory effort before the capnogram.

4.1 Presence of Supplemental O_2

An important result obtained from tests conducted on the bench was a better understanding of the effect of viscosity of the sampling gas on the functioning of the pneumatic system of the sidestream capnometer. Different gases are involved during inspiration and expiration. Any transition between them produces a change in the viscosity of the sampling gas. This change alters the flow profile of the CO_2 signal, producing faulty flow measurements. A feedback system based on faulty readings is ineffective. This deterioration in the performance of the sampling system will impact the

shape of the CO_2 signal and might affect patient diagnostics. A falsely elevated sampling flow would result in an upslope in the capnogram that would be steeper than normal. Similarly, an erroneously low sampling flow would produce a capnogram with an unusually gradual descending limb. The sampling flow signal from one of the clinical data files is shown in Figure 55. A possible solution might be to take into account the sampling pressure, in addition to the pressure drop across the flow meter, while activating feedback control. An absolute pressure value might help reflect the true condition better than a differential pressure reading.

Another observation in the presence of supplemental O_2 was a false elevation in the amplitude of the sampling pressure signal. In order to test if a correlation can still be drawn between the sampling pressure and the true nasal pressure signals, the standard deviation of the two signals was determined in every minute of each data file collected during the colonoscopy study and correlated. The results are displayed in Figure 56. It can be concluded that there is no correlation between the signals. This establishes that the amplitude of sampling pressure does not give useful information about the size of the breath when supplemental O_2 is in use.

In the ICU and OR where capnography is used most, how important is the breath size? In these clinical settings, it is most important for the patient to keep breathing continuously. Normal O_2 consumption is about 250 mL per minute. [30] Hence, receiving 250 mL of O_2 per minute is sufficient to maintain healthy blood oxygen saturation. The normal minute volume in humans is 6 LPM or 100 mL/s. The tidal volume is usually set to the same level when the patient is mechanically ventilated. When 100% supplemental O_2 is given, the patient receives 100 mL of O_2 per second. This implies that in about 3

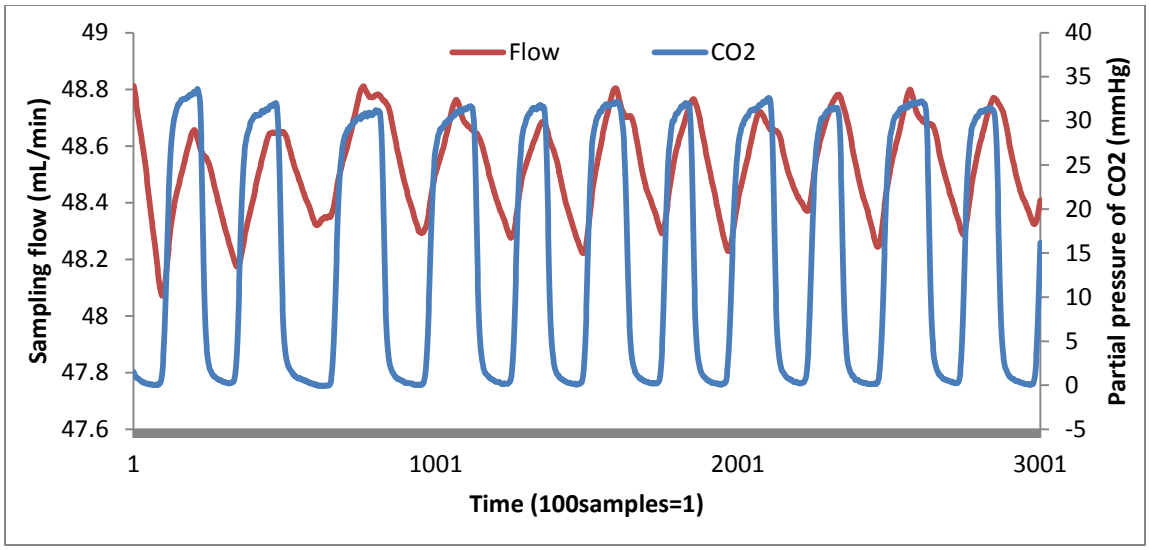

Figure 55: Changes in sampling flow with each breath at 5 LPM of supplemental O_2. O_2 is the first gas to be sampled at the beginning of expiration as the dead space is cleared. The increased viscosity of the sampling gas produces an increase in the sampling flow as indicated by the upward swing on the brown line. Once the pump senses an increase in its load due to the presence of the viscous gas, it slows down to contain the sampling flow. This is reflected by the downward swing coinciding with the end of expiration. The cycle repeats.

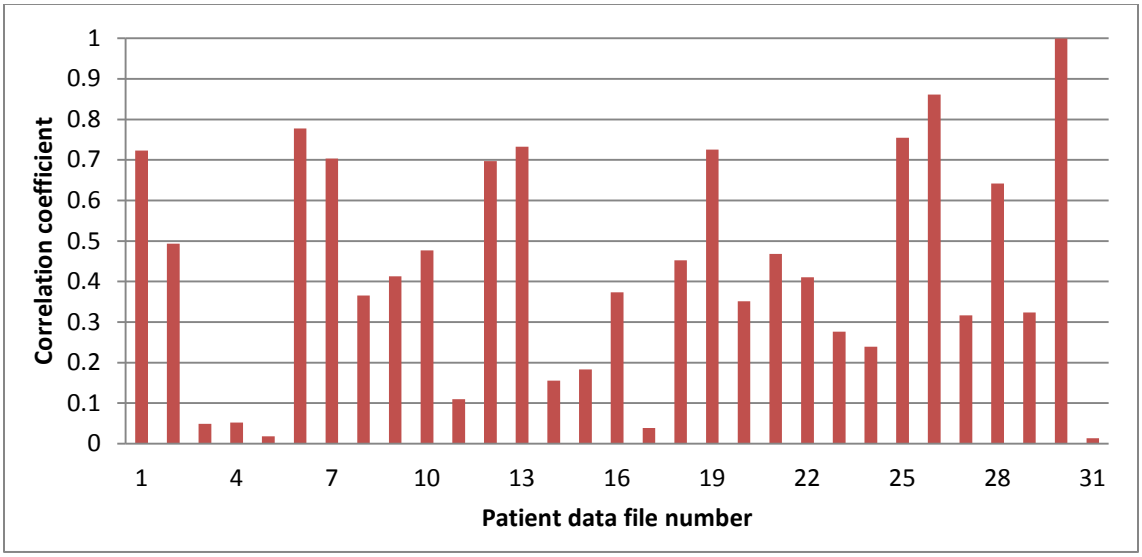

Figure 56: Correlation between nasal pressure and sampling pressure. The average correlation between the signals was 43%, indicating that the sampling pressure signal cannot be used to infer breath size.

seconds, the patient meets his O_2 requirement for a minute. So even if he is taking only 1 or 2 breaths a minute, a normal SpO_2 is maintained and projected by a pulse oximeter. Only sustained apnea can cause the blood O_2 level to fall enough for the pulse oximeter to sound an alarm. When the sampling pressure signal was considered independently, it recorded 26 true apneic events. Of these, the SpO_2 dropped below 90% in only 19% of the cases. In such a situation where apnea is not detected by a pulse oximeter, monitoring of breath rate by a more reliable technology takes precedence over monitoring of breath size. This implies that the performance of a signal in detecting a breath accurately is more critical than determining the size of the breath. Hence, it can be said that the sampling pressure signal accomplishes the more important task of detecting breaths accurately.

4.2 Utility of Sampling Pressure Signal

As determined in Chapter 2, the sampling pressure signal was advanced by 549 ± 14 samples in order to be aligned with the CO_2 signal which, at a sampling rate of 100 Hz, is 5.49 ± 0.14 seconds. Added to this is the fact that the sampling pressure signal shows deflections during both inspiration and expiration, unlike the capnogram that reflects only the patient's expiratory status. Therefore, the pressure signal would detect apnea earlier and also indicate a respiratory effort before the capnogram does. Moreover, the signal was found to have an accuracy of 99%, specificity of 100%, and sensitivity of 96%. These prove that the sampling pressure is a more accurate and reliable source of respiratory monitoring than the capnogram.

An important auxiliary result that was achieved was the detection of supplemental O_2 using the sampling pressure signal. This feature could help build an accurate and

useful clinical decision support system. While a pulse oximeter could take a few minutes to detect blood O_2 desaturation, [31] the sampling pressure signal could potentially forewarn the clinician about its possible occurrence. Future work could focus more on this area and development of such an application which could be used in a clinical setting.

REFERENCES

1. Ballester, E, Badia JR, Hernández L, Farré R, Navajas D, Montserrat JM. Nasal prongs in the detection of sleep-related disordered breathing in the sleep apnoea/hypopnoea syndrome. Eur Respir J 1998; 11(4): 880-3

2. Sam E Farish and Paul S Garcia. Capnography Primer for Oral and Maxillofacial Surgery: Review and Technical Considerations. J Anesth Clin Res 2013; 4(3): 295

3. J. S. Gravenstein, Michael B. Jaffe, Nikolaus Gravenstein, David A. Paulus. Capnography. 2nd ed. Cambridge: Cambridge University Press, 2011

4. Technical Staff – Respironics , Respironics LoFlo™ and Oridion Microstream® Technologies Contrasted, Respironics Whitepaper, 2003

5. Jaffe, Michael B., Sidestream Gas Monitoring with a Detachable Sample Cell – The LoFl System, Respironics Whitepaper, 2003.

6. The LoFlo™ System Technical Staff – Respironics , 21st Century CO2 Technology Sidestream Monitoring, Respironics Whitepaper, 2007

7. Michael B. Jaffe, Flow Measurement with Respironics Novametrix Series 3 Flow Sensors, Respironics Whitepaper, 2002

8. Cook TM, Woodall N, Harper J, Benger J. Major complications of airway management in the UK: results of the Fourth National Audit Project of the Royal College of Anaesthetists and the Difficult Airway Society. Part 2: intensive care and emergency departments. BJA 2011; 106(5):632-42

9. Aalexandre Yazigi, Carine Zeeni, Freda Richa, Viviane Chalhoub, Ghassan Sleilaty and Roger Noun. The accuracy of non-invasive nasal capnography in morbidly obese patients after bariatric surgery. Middle East J Anesthesiol 2007; 19 (3): 483-494

10. Bennett J, Petersen T, Burleson J. Capnography and ventilatory assessment during ambulatory dentoalveolar surgery. JOMI 1997; 55:925-6

11. Krauss B, Hess DR. Capnography for procedural sedation and analgesia in the

emergency department. Ann Emerg Med 2007; 50(2):172-81

12. Deitch K, Chudnofsky CR, Dominici P. The utility of supplemental oxygen during emergency department procedural sedation with propofol: a randomized, controlled trial. Ann Emerg Med 2008; 52(1):1-8

13. Rosenblatt WH, Kharatian A. Capnography: never forget the false-positives! Anesth Analg 1991; 73(4):509-10.

14. Lawless ST. Crying wolf: false alarms in a pediatric intensive care unit. Crit Care Med 1994; 22(6):981-5.

15. Chambrin, M.-C., Ravaux, P., Calvelo-Aros, D., Jaborska, A., Chopin, C. & Boniface, B. Multicentric study of monitoring alarms in the adult intensive care unit (ICU): a descriptive analysis. Intensive Care Med 2004; 25: 1360-6.

16. Bhavani-Shankar, Moseley H, Kumar AY, Delph Y. Capnometry and anaesthesia, Can J Anaesth 1992; 39(6): 617-32

17. Jacqueline D'Mello, Manju Butani. Capnography. Indian J Anesth 2002; 46 (4):269-278

18. Imanaka H, Nishimura M, Takeuchi M, Kimball WR, Yahagi N, Kumon K.. Autotriggering caused by cardiogenic oscillation during flow-triggered mechanical ventilation. Crit Care Med 2000; 28(2): 402-7

19. Guyatt AR, Parker SP, McBride MJ. Measurement of human nasal ventilation using an oxygen cannula as a pitot tube. Am J Respir Crit Care Med 1982; 126(3):434-8.

20. Thurnheer, R., X. Xie, and K.E. Bloch. Accuracy of nasal cannula pressure recordings for assessment of ventilation during sleep. Am J Respir Crit Care Med 2001; 164(10.1): 1914-9

21. Jaffe, Michael B., Mainstream or Sidestream Capnography? Technical Considerations. Respironics Whitepaper, 2002.

22. Steven J. Heitman, Raj S. Atkar, Eric A. Hajduk, Richard A. Wanner, and W. Ward Flemons. Validation of nasal pressure for the identification of apneas/hypopneas during sleep. Am J Respir Crit Care Med 2002; 166(3): 386-91

23. Kate E. Crowley, Shantha M.W. Rajaratnam, Steven A. Shea, Lawrence J. Epstein, Charles A. Czeisler, Steven W. Lockley. Evaluation of a Single-Channel Nasal Pressure Device to Assess Obstructive Sleep Apnea Risk in Laboratory and Home Environments. J Clin Sleep Med. 2013; 9(2): 109–16.

24. Jean-Jacques Hosselet, Robert G. Norman, Indu Ayappa, and David M. Rapoport. Detection of Flow Limitation with a Nasal Cannula/Pressure Transducer System. Am J Respir Crit Care Med 1998; 157: 1461–7

25. Indu Ayappa, Robert G Norman, Ana C Krieger, Alison Rosen, Rebecca L O'Malley and David M Rapoport. Non-Invasive Detection of Respiratory Effort-Related Arousals (RERAs) by a Nasal Cannula/Pressure Transducer System. Sleep 2000; 23(6): 763-71

26. Lourdes Herna´ndez, Eugeni Ballester, Ramo´n Farre, Joan Ramo´n Badia, Rafael Lobelo, Daniel Navajas and Josep Maria Montserrat. Performance of Nasal Prongs in Sleep Studies- Spectrum of Flow-Related Events. Chest 2001; 119(2): 442-51

27. Norman RG, Ahmed MM, Walsleben JA and Rapoport DM. Detection of respiratory events during NPSG: nasal cannula/pressure sensor versus thermistor. Sleep 1997; 20(12):1175-84

28. Sériès F, Marc I. Nasal pressure recording in the diagnosis of sleep apnoea hypopnoea syndrome. Thorax 1999; 54(6):506-10.

29. Rühle KH, Fahrner A, Randerath W. Evaluating oronasal flow with temperature (thermistor) and obstructive pressure (prongs). Pneumologie 2001; 55(1):4-6.

30. Scott D. Weingart, Richard M. Levitan. Preoxygenation and prevention of desaturation during emergency airway management. Ann Emerg Med 2012; 59(3):165-75.

31. H. Guggenberger, G. Lenz, R. Federle. Early detection of inadvertent oesophageal intubation: pulse oximetry vs. capnography. Acta Anaesthesiol Scand 1989; 33: 112–115.